NAVAL PROVING GROUND

DAHLGREN, VIRGINIA

REPORT NO. 2-46

BALLISTIC SUMMARY - PART I
THE DEPENDENCE OF LIMIT VELOCITY ON PLATE THICKNESS AND OBLIQUITY AT LOW OBLIQUITY.

1 March 1946

DISCLAIMER NOTICE

UNCLASSIFIED

NAVAL PROVING GROUND
DAHLGREN, VIRGINIA

Captain David I. Hedrick, USN
Commanding Officer

Captain K. M. McLaren, USN
Ordnance Officer

NPG Report No. 2-46

APPROVED FOR PUBLIC RELEASE,
DISTRIBUTION UNLIMITED.

BALLISTIC SUMMARY - PART I
THE DEPENDENCE OF LIMIT VELOCITY ON PLATE THICKNESS
AND OBLIQUITY AT LOW OBLIQUITY.

CLASSIFICATION (CANCELLED) Unclassified NavOrd ltr 0652/1178 PAH
ON 8/31/76 (DATE) B. Broyles (SIGNATURE) (RANK) 5511 10/31/73

A. V. HERSHEY
Lieutenant, USNR

APPROVED FOR PUBLIC RELEASE,
DISTRIBUTION UNLIMITED.

UNCLASSIFIED

1 March 1946

NPG Report No. 2-46.

BALLISTIC SUMMARY - PART I
THE DEPENDENCE OF LIMIT VELOCITY ON PLATE THICKNESS
AND OBLIQUITY AT LOW OBLIQUITY.

1. For some years the Naval Proving Ground has been assiduously engaged in the study of the penetration of armor by projectiles. Pursuance of this work to conclusive results must be predicated upon well substantiated theories defining the performances of the materials involved under the various possible conditions.

2. Particularly necessary in the more immediately practical field of armor study and evaluation is the need for dependable plate penetration charts or tables. In 1943 Lieut. A. V. Hershey, USNR was assigned the task of preparing such charts. In prosecution of the assigned task he conducted an exhaustive study, employed for the first time new methods of attack and developed new theories concerning the phenomena incident to the penetration of plates by projectiles.

3. During the latter years of World War II, Lieut. Hershey prepared a series of nine reports which are being published by the Naval Proving Ground under titles as follows:

(1) ANALYTICAL SUMMARY. PART I. THE PHYSICAL PROPERTIES OF STS UNDER TRIAXIAL STRESS.

Object: To summarize the available data on the physical properties of Class B Armor and STS under triaxial stress.

(2) ANALYTICAL SUMMARY. PART II. ELASTIC AND PLASTICS UNDULATIONS IN ARMOR PLATE.

Object: To analyse the propagation of undulations in armor plate; to summarize previous analytical work and to add new analytical work where required in order to complete the theory for ballistic applications.

(3) ANALYTICAL SUMMARY. PART III. PLASTIC FLOW IN ARMOR PLATE.

Object: To analyse the plastic flow in armor plate adjacent to the point of impact by a projectile.

(4) ANALYTICAL SUMMARY. PART IV. THE THEORY OF ARMOR PENETRATION.

Object: To summarize the theory of armor penetration in its present state of development, and to develop theoretical functions which can be used as a guide in the interpretation of ballistic data.

(5) BALLISTIC SUMMARY. PART I. THE DEPENDENCE OF LIMIT VELOCITY ON PLATE THICKNESS AND OBLIQUITY AT LOW OBLIQUITY.

Object: To compare the results of ballistic test with the prediction of existing formulae, and with the results of theoretical analysis; to find the mathematical functions which best represent the fundamental relationship between limit velocity, plate thickness, and obliquity at low obliquity.

(6) BALLISTIC SUMMARY. PART II. THE SCALE EFFECT AND THE OGIVE EFFECT.

Object: To determine the effect of scale on ballistic performance, and to correlate the projectile nose shape with the results of ballistic test.

(7) BALLISTIC SUMMARY. PART III. THE WINDSHIELD EFFECT, AND THE OBLIQUITY EFFECT FOR COMMON PROJECTILES.

Object: To analyse the action of a windshield during impact, and to develop mathematical functions which best represent the ballistic performance of common projectiles.

(8) BALLISTIC SUMMARY. PART IV. THE CAP EFFECT, AND THE OBLIQUITY EFFECT FOR AP PROJECTILES.

Object: To determine the action of a cap during impact, and to develop mathematical functions which best represent the ballistic performance of AP projectiles.

(9) BALLISTIC SUMMARY. PART V. THE CONSTRUCTION OF PLATE PENETRATION CHARTS OR TABLES.

Object: To summarize the results of analysis in the form of standard charts or tables.

4. The opinions and statements contained in these reports are the expressions of the author, and do not necessarily represent the official views of the Naval Proving Ground.

David I. Hedrick

DAVID I. HEDRICK
CAPTAIN, U. S. NAVY
COMMANDING OFFICER

PREFACE

AUTHORIZATION

The material in this report has been basic to the construction of plate penetration charts. It was authorized by BuOrd letter NP9/A9 (Re3) dated 9 January 1943.

OBJECT

To compare the results of ballistic test with the predictions of existing formulae, and with the results of theoretical analysis; to find the mathematical functions which best represent the fundamental relationship between limit velocity, plate thickness, and obliquity at low obliquity.

SUMMARY

The various empirical formulae which are basic to BuOrd Sk 78841, to quality control charts, and to NPG Sk 650 are compared with the results of ballistic test. The basic theorems and assumptions of a new theoretical analysis of armor penetration are summarized, and the results of the theory are compared with the results of ballistic test. New functions are given, which best represent the fundamental relationship between limit velocity, plate thickness, and obliquity at low obliquity. The functions apply specifically to 3" AP M79 projectiles against ductile Class B Armor or STS of 115,000 $(lb)/(in)^2$ tensile strength at 15°C, in a range of e/d from .004 to 2.0.

CONTENTS

LIST OF FIGURES

LIST OF TABLES

I INTRODUCTION

Terminal ballistics in modern naval warfare have covered a wide range of impact conditions, from bomb impacts on thin deck plate at one extreme to projectile impacts on heavy turret plates at the other. The variables which influence ballistic performance in the range of service interest have been the subject of recent systematic investigations, References (1) to (10) (Page 31).

Variables which influence the ballistic properties of armor plate are the thickness and size of the plate, the tensile strength or the hardness distribution, the temperature, the microstructure, the chemical composition and the homogeneity of the plate material. Variables which influence the ballistic properties of a projectile are the diameter and mass of the projectile, the distribution of mass between the body, the cap, the windshield, and the driving band or carrier, the distribution of hardness in each of these component parts, and the geometrical shape of each part. Variables which define the conditions of impact are the striking velocity, the obliquity, and the yaw. Variables which define the results of impact are the depth of penetration in an incomplete penetration, or the remaining velocity in a complete penetration, the type of plate failure, and the extent of projectile damage. From the results of impact may be estimated the limit velocity, or that striking velocity which would just put the major portion of the projectile through the plate with zero remaining velocity.

The mass and diameter of the projectile, the thickness of the plate, the obliquity of impact and the limit velocity may be classified as primary ballistic variables, while the design of the projectile and the quality of the plate may be classified as secondary variables. The fundamental relationships between the primary variables are the subject of the present summary. The scale effect, the ogive effect, the cap effect, the windshield effect, and the ricochet effect will be the subject of later summaries.

The fundamental relationships between the primary variables would be best represented by the terminal ballistics for nondeforming monobloc projectiles in homogeneous plates of constant ductility. The effects of secondary variables could then be assessed by a comparison between the experimental results of actual performance and the predicted results for ideal performance. The fundamental relationships between the primary variables would be established by a systematic program of limit determinations on armor steel of completely controlled quality. Armor plate is the product of manufacturing processes, however, which leave the plate material in a thermodynamically unstable state. The ballistic performance of armor is subject to statistical fluctuations which are often capricious, and a very large sample of ballistic data would be required in order to establish with precision the ideal average performance. The fundamental relationships between the primary variables would also be established by an exact theoretical analysis of the mechanism of armor penetration. An exact theory would involve such complicated computations, however, that the analysis is beyond the reach of the solitary analyst.

There are available, nevertheless, a series of 170 precise limit determinations with undeformed 3" monobloc projectiles, all with nearly the same ogive. These are supplemented by additional ballistic data on bombs and small caliber monobloc projectiles which extend the range of the data. Details of the ballistic data have been released in previous reports, References (1) to (10), but the results are summarized in the present report. A semiquantitative theoretical analysis of the mechanics of armor penetration has been completed and the details will be released in later reports. The basic assumptions of the theoretical analysis are summarized in the present report. The most likely relationships between the primary variables have been derived from the ballistic data, with the theoretical analysis as a guide to the proper choice of functions. The experimental relationships are represented in Figures (1) to (22) by Curve I.

II EMPIRICAL FORMULAE

Various empirical formulae have been used in the past to express relationships between the limit velocity, the plate thickness, and the obliquity. One of the most important has been the deMarre formula, which was used for many years by the U. S. Navy and is still used by the British. The deMarre formula is defined in terms of the limit velocity v_L, the plate thickness e, the obliquity θ, the projectile diameter d, and the projectile mass m by the equation

$$v_L = \frac{4' e^{.70} d^{.75}}{m^{.50}} \sec^{\frac{3}{2}} \theta \qquad (1)$$

in which A' is a constant.* A curve to represent the deMarre formula is compared with the experimental curve in Figure (1). The deMarre formula does not conform to the conditions of dimensional similitude, and was therefore discarded by the U. S. Navy in 1936 in favor of a new formula.

Dimensional analysis was first applied to armor penetration in 1927 by Thompson at the Naval Proving Ground. An elementary dimensional analysis leads to a combination of the ballistic variables into a single parameter, which is expressible, for steel of constant quality, as a function of the ratio e/d, and the obliquity θ. The results of dimensional analysis are stated analytically by the equation

$$\frac{m^{\frac{1}{2}} v_L \cos\theta}{e^{\frac{1}{2}} d} = F(e/d, \theta) \tag{2}$$

The function $F(e/d, \theta)$ is called the plate penetration coefficient. The dimensional analysis does not determine the actual form of the function $F(e/d, \theta)$, but merely states that it exists, and the actual form must be found by experimental test.

On the basis of data available in 1932 the Naval Proving Ground chose for the function $F(e/d, \theta)$ a formula expressed by the equation

$$F(e/d, \theta) = 6\left(\frac{e}{d} - 0.45\right)(\theta^2 + 2000) + 40000 \tag{3}$$

which is basic to BuOrd Sk. 78841 and is still in use by the U. S. Navy. Equation (3) is an excellent representation of the data available in 1932. It is now known to be valid, however, for modern armor at only one point, and at that point only for projectiles which are similar in design to the 8" AP Mk 11-1 projectile. Equation (3) is plotted in Figure (2) for comparison with the experimental curves. Equation (3)

*The deMarre coefficient for a plate is the ratio between the value of A' for the plate and the value of A' for nickel steel.

corresponds to a family of straight lines in a plot of $F(e/d,\theta)$ vs e/d, whereas the actual ballistic data fall on curves. The straight lines for various obliquities all intersect at the same point, whereas the actual curves at low obliquity do not intersect. The errors in Equation (3) are believed to arise from an improvement in armor quality which may have occurred in 1930, at the same time that the prevailing obliquity of test at the Naval Proving Ground was shifted from 0° to 30°.

The production control of armor is facilitated at the firing range by the maintenance of control charts, in which the limit velocity v_L is plotted directly against the plate thickness e. Separate charts are used for each combination of projectile design, armor class, and test obliquity. Straight lines are drawn in the charts to represent average quality. A straight line in a plot of limit velocity against plate thickness corresponds to a plate penetration coefficient which is given by an equation of the form

$$F(e/d,\theta) = c_1\left(\frac{e}{d}\right)^{-\frac{1}{2}} + c_2\left(\frac{e}{d}\right)^{+\frac{1}{2}} \tag{4}$$

in which the coefficients c_1 and c_2 vary from chart to chart. Equation (4) is plotted in Figure (3) for comparison with the experimental curve. Inspection of the figure shows that the straight line may be used with success over a limited range of plate thickness, but cannot be safely extrapolated.

III BALLISTIC PARAMETERS

The analysis of armor penetration is aided by the use of a variety of ballistic parameters. The impact parameter F_S, the plate penetration coefficient $F(e/d,\theta)$, and the residual velocity function F_R may all be defined in terms of the projectile mass m, the projectile diameter d, the plate thickness e, the obliquity θ, the striking velocity v_S, the limit velocity v_L, and the remaining velocity v_R, by the equations

$$F_S = \frac{m^{\frac{1}{2}} v_S \cos\theta}{e^{\frac{1}{2}} d}$$

$$F(e/d,\theta) = \frac{m^{\frac{1}{2}} v_L \cos\theta}{e^{\frac{1}{2}} d}$$

$$F_R = \frac{m^{\frac{1}{2}} v_R \cos\theta}{e^{\frac{1}{2}} d}$$

The impact parameter F_S is a function only of independent variables which define the conditions of impact. The impact parameter F_S is therefore also an independent variable. The plate penetration coefficient $F(e/d,\theta)$ is an explicit function of the limit velocity, which is derived from the results of test, and is therefore a dependent variable. The plate penetration coefficient $F(e/d,\theta)$ is an implicit function of e/d, θ, and secondary variables. The residual velocity function F_R is an explicit function of the remaining velocity, and is therefore, also a dependent variable. The residual velocity function F_R is an implicit function of F_S, e/d, θ, and secondary variables. These parameters are convenient to use in the representation of ballistic data, since they are directly proportional to velocity, and do not vary rapidly with plate thickness or obliquity.

Of more fundamental significance are the impact energy parameter U_S, the limit energy function $U(e/d,\theta)$, and the residual energy function U_R, which are defined in terms of F_S, $F(e/d,\theta)$, and F_R by the equations

$$U_S = \left(\frac{e}{d}\right) F_S^2$$

$$U\left(\frac{e}{d},\theta\right) = \left(\frac{e}{d}\right) F^2\left(\frac{e}{d},\theta\right) = \frac{m v_L^2 \cos^2\theta}{d^3}$$

$$U_R = \left(\frac{e}{d}\right) F_R^2$$

These parameters are proportional to the kinetic energy of the projectile at normal obliquity.

Another series of parameters, which are useful in the interpretation of absorption data, are the parameters F_S^2, $F^2(e/d,\theta)$ and F_R^2. The parameter $F^2(e/d,\theta)$ is proportional to the average pressure on the projectile during impact at normal obliquity.

Ballistic performance may be interpreted with equal validity in terms of any one of the three functions $F(e/d,\theta)$, $F^2(e/d,\theta)$ or $U(e/d,\theta)$. The projectile mass in the functions is expressed in (lb), the projectile diameter is given in (ft), the plate thickness in (ft) and the velocity of the projectile in (ft)/(sec).

IV SEMIEMPIRICAL FORMULAE

An elementary theoretical analysis of armor penetration was made in 1941 by Bethe. It was assumed in Bethe's theory that the final energy required to make a hole through a plate is the same, regardless of the penetration cycle, and that the plastic energy in a projectile impact is therefore the same as the plastic energy required to expand slowly a hole of uniform diameter in the plate. Bethe's theory leads to a direct proportionality between the energy of penetration and the plate thickness, and may be represented analytically by an equation of the form

$$U\left(\frac{e}{d},\theta\right) = B\left(\frac{e}{d}\right) \qquad (\theta = 0°)$$

in which B is a constant of proportionality. This equation is equivalent to a constant $F(e/d,\theta)$ independent of e/d, and is therefore contrary to the ballistic data.

It was recognized in 1942 at the Naval Proving Ground that the ballistic data at values of e/d as low as 0.5 are in better agreement with an equation of the form

$$U(e/d,\theta) = -A + B\left(\frac{e}{d}\right) \qquad (\theta = 0°)$$

in which the constant correction term $-A$ was attributed to the formation of a coronet on the face of the plate and a star crack on the back. Extensive use has been made of this equation in the interpretation of the ballistic data for light armor.

The limit energy function $U(e/d,\theta)$ can never be negative, and must vanish at $e/d = 0$. In order to find an equation which is valid over a still wider range of e/d, the term $-A$ was replaced in 1944 by a function of e/d, which approaches a constant at high e/d but becomes zero at $e/d = 0$. The equation which was chosen to represent $U(e/d,\theta)$ at normal obliquity was

$$U(e/d,\theta) = -A\tanh(\Gamma\frac{e}{d}) + B(\frac{e}{d}) \qquad (\theta = 0°)$$

with A, B, Γ all constant.

The ballistic data for other obliquities than normal contain overwhelming evidence that, contrary to the predictions of Equations (1) or (3), the limit energy function $U(e/d,\theta)$ decreases, at obliquities less than 30°, with increase in obliquity and is, in fact, nearly proportional to $\cos\theta$. The limit energy function $U(e/d,\theta)$ would be accurately proportional to $\cos\theta$ if the plastic energy of penetration were proportional to the volume of impact hole. The limit energy function $U(e/d,\theta)$ goes through a minimum at an obliquity near 45°, and increases with increase in obliquity at obliquities greater than 45°.

The equation which was finally chosen in 1944 to represent $U(e/d,\theta)$ at low obliquity was

$$U(e/d,\theta) = \{-A\tanh(\Gamma\frac{e}{d}) + B(\frac{e}{d})\}\Theta\cos\theta \qquad (5)$$

in which Θ is a function of obliquity. In the case of a 3" AP M79 projectile against STS with a tensile strength of 115000 $(lb)/(in)^2$, the parameters A, B, Γ and Θ were given by the equations

$$A = (4.3)(10^8) \qquad B = (28.2)(10^8) \qquad \Gamma = 5.7 \qquad (6)$$

$$\Theta = 1 + \frac{5}{\sqrt{\pi}}\int_{-\infty}^{3.6(\frac{1}{2}-\cos\theta)} e^{-\beta^2}\,d\beta - .03\sin^2\theta \qquad (7)$$

The obliquity function θ at low obliquity was based on the ballistic data for 3" AP M79 projectiles, and at high obliquity on the ballistic data for 6" Comm Mk 27 projectiles.

Equations (5) and (7) are basic to NPG Sk 650. Plate penetration coefficients and obliquity functions to represent Equations (5) and (7) are plotted in Figures (4) and (10) for comparison with experimental curves.

The limit energy function defined by Equation (5) becomes a linear function of e/d at hypervelocity, whereas the actual limit energy function for nondeforming projectiles varies at a faster rate with e/d. The Princeton University Station has summarized the terminal ballistics of small caliber projectiles at hypervelocity by an empirical equation of the form

$$U(e/d, \theta) = B'\left(\frac{e}{d}\right)^n \qquad (\theta = 0°) \qquad (8)$$

in which the exponent n is equal to 1.26 for monobloc projectiles, and the coefficient B' is equal to $(24.0)(10^8)$ for uncapped APC projectiles. The Princeton formula is represented by Curve VI in Figure (9).

V THEORETICAL FUNCTIONS

The theory of armor penetration in its present state of development may be summarized by a set of qualitative theorems which describe the major phenomena in the mechanism of penetration.

The theoretical analysis of armor penetration consists in the recognition of the various forms of energy which are taken up by the armor during impact, and the evaluation of these forms of energy in terms of known relationships between stress, strain, and rate of strain.

The stress-strain relationships for slow isothermal flow are all similar in the three limiting cases of shear, tension and compression. The stress-strain relationships for intermediate cases may be found from the limiting cases by interpolation. There appears to be no evidence that armor steel is anisotropic, although it is often inhomogeneous. The principal axes of stress are probably therefore collinear with the principal axes of strain rate. The ratios between the principal components of stress are functions of the ratios between the principal components of strain rate. The components of stress for rapid plastic flow are greater than the components of stress for slow plastic flow, by a factor which varies slowly with the strain rate. The shear stress in armor steel decreases with increase in temperature, and increases with increase in normal pressure.

The stress-strain curve for shear, during isothermal flow, rises continuously as the strain increases. The temperature, during adiabatic flow, rises also as the strain increases. The stress for adiabatic flow is therefore less than the stress for isothermal flow. The stress-strain curve for shear, during adiabatic flow, passes through a maximum as the strain increases. A homogeneous strain in the medium is unstable with respect to a localized strain wherever the strain in the medium exceeds the strain for maximum shear stress, and the medium may rupture by shear. The transition from homogeneous strain to localized strain is probably precipitated by the presence of inhomogeneities in the medium, and may be retarded by their absence.

The work done on unit volume of the medium is not a single valued function of the final strain, but depends also on the path of deformation. Pure compression, with simultaneous rotation of the principal axis of compression through 180°, produces nearly the same final strain as pure shear with stationary principal axes of strain, yet the plastic work is nearly twice as great.

A disturbance in the interior of a solid medium is propagated by two waves which move with different velocities. The leading wave is a compressional or longitudinal wave, while the trailing wave is an equivoluminal or transverse wave. The velocity of propagation of the longitudinal wave is determined primarily by the bulk modulus of the medium and remains finite for any strain. The velocity of propagation of the transverse wave is derived from the stress-strain curve for shear, and decreases to zero as the strain in the medium approaches the strain for maximum stress.

A longitudinal wave in a solid medium is not isotropic. Transverse and longitudinal waves are therefore both reflected when a longitudinal wave reaches a free surface*. The principal axes of stress at a free surface are always parallel to the surface, and the principal component of stress normal to the surface is zero. A line in the medium which

*A free surface is any boundary surface to which no external forces are applied.

was initially orthogonal to a free surface continues to be orthogonal during any distortion of the free surface.

A transverse undulation is created in a plate at the point of impact, and is propagated rapidly away over the surface of the plate. If the undulation is elastic, it is maintained by a force, which increases with increase in both the velocity and the displacement of the plate at the point of application of force. The undulation in the limiting case of a thin membrane is propagated at a finite rate only in the presence of a tension stress, which is built up by the undulation itself. The undulation in the limiting case of a thick plate is propagated by a flexual rigidity, which is independent of the amplitude of undulation. Formulae for elastic undulations in a thin membrane and a thick plate may be derived, and combined into a simple formula, whose algebraic form is consistent with direct experiments on elastic undulations in plates of intermediate thickness.

The pressure on the nose of the projectile during a limit impact is more than the plate material can stand without plastic flow. The plate material in the path of the projectile is forced outward toward the nearest free surface, and the plate is increased in thickness around the point of impact. The volume of plate material in the path of the projectile is directly proportional to the plate thickness and inversely proportional to the cosine of the obliquity. The amount of plastic flow is determined by the volume of plate material in the path of the projectile, but the distribution of plastic flow is determined by the proximity of the free surfaces. The plastic flow is thus concentrated near the point of impact in a thin plate, but is spread out to a greater radius in a thick plate. The plastic flow is symmetric about an impact at normal obliquity, but is concentrated around the sides nearest to the plate normal at other obliquities. The plastic energy in a limit impact at low obliquity is almost inversely proportional to the cosine of the obliquity but not quite, because the distribution of plastic flow changes with obliquity. The plastic energy in a limit impact at high obliquity on the other hand increases more rapidly with obliquity because of projectile ricochet.

The velocity of propagation of a longitudinal wave in the medium is always many times greater than the velocity of the projectile. The velocity of propagation of a transverse wave is initially also greater than the velocity of the projectile, but decreases, during impact, as the plastic flow proceeds. Multiple reflections of the transverse waves between the faces of a thin plate maintain the medium near the point of impact in a state of equilibrium. Dynamics in a thin plate are only important at the outer radius of the transverse undulation. The transverse waves in a thick plate, however, are not quite able to maintain the medium in a state of equilibrium. The velocity of propagation of a transverse wave in a thick plate diminishes toward the point of impact, and is zero at a distance of one tenth caliber from the surface of the impact hole. The transverse waves originate at the free surfaces of the plate and move inward, but there is a zone next to the impact hole which is reached only by longitudinal waves. The medium in this zone is maintained in a state of steady irrotational* flow.

The plastic flow has been analyzed for the two limiting cases of a thin plate and a thick plate.

The tension-extension relationship in a thin membrane is the analog of the load-elongation relationship in a tensile bar. The tension in the membrane is a maximum at the same value of the uniaxial component of strain as the load in the tensile bar. The membrane thins down and ruptures whenever the strain in the membrane reaches the critical strain for maximum tension. A pointed projectile ruptures a membrane almost on contact, and forms a star crack. Stress concentration at the outer ends of each branch of the star crack propagates the crack with little expenditure of energy. The plastic energy of penetration is nearly all expended on distortion of the petals of the star. The petals are changed during impact, from sectors of a plane disc into segments of a circular cylinder. The plastic energy in a membrane is proportional to the thickness of the membrane.

A thin plate of finite thickness does not crack until the projectile has penetrated nearly to the back of the plate. Plastic energy is required to bring the plate to the point of fracture.

---

*Irrotational flow is any flow in which the velocity may be expressed at every point as the gradient of a scalar function. The streamlined flow around a projectile in a perfect fluid would be irrotational.

A theoretical curve has been plotted in Figures (5) and (7) to represent the thin plate theory. The theoretical curve is based on the following simplifications:

(a) The energy required to crack the plate is assumed to be proportional to the imbedded volume of the projectile with the tip of the nose just at the back of the plate. The average pressure on the projectile before fracture of the plate is assumed to be equal to the average pressure in the equilibrium expansion of a hole of uniform diameter. The thickness of the plate near the point of impact, just at fracture, is assumed to be equal to the thickness of the plate near a hole of uniform diameter.

(b) The energy required to push back the petals after fracture is assumed to be proportional to the plate thickness.

(c) The energy delivered to the transverse undulation by the projectile is assumed to be the same as the energy in an elastic undulation with the force concentrated at a point.

The theoretical curve is lower than the experimental curve, but is similar in shape. There have been no ballistic tests on STS at e/d less than 0.04, but there has been one limit determination on mild steel at $e/d = 0.004$. The theoretical analysis is consistent with the results on mild steel, and has therefore been used as a guide to the limiting curve for STS at very low e/d. The plastic energy, per unit thickness of plate, theoretically approaches a constant limit as e/d goes to zero, but the elastic energy per unit thickness increases slowly. The plate penetration coefficient $F(e/d,\theta)$ has therefore been assumed to increase with decrease in e/d at values of e/d less than 0.02.

Fractures in a thick plate occur in a central zone next to the impact hole where the strain in the medium is greater than the strain for maximum shear stress. Faults appear in the interior of the plate and cracks appear on the faces of the plate. The surfaces of the cracks coincide with the surfaces of maximum shear stress in the plate.

If the medium did not work harden, the velocity of propagation for transverse waves would be zero, and the flow would be irrotational throughout. The plastic flow adjacent to the surface of the plate is maintained, by the transverse waves, in a state of equilibrium with one component of stress equal to zero. Approximately half of the plastic work on the medium in a plate of caliber thickness is actually performed under conditions of irrotational flow, and half is performed under conditions of equilibrium flow. The energy required by irrotational flow is greater than the energy required by equilibrium flow. The principal axes of strain rate rotate in the zone of irrotational flow as the projectile moves through the plate, but the principal axes of strain rate at the free surfaces are held fixed in the medium, and plastic flow extends to a greater distance from the point of impact in the zone of irrotational flow.

The plate thickness at the rim of the impact hole should increase during impact by a nearly constant amount independent of plate thickness in the limiting case of pure irrotational flow, but the amount of increase should be proportional to plate thickness in the limiting case of pure equilibrium flow. The thickness at actual impact holes is in fact nearly equal to the thickness for pure irrotational flow, but increases slightly with increase in plate thickness.

Theoretical curves have been plotted in Figures (5), (7), (9) and (10) to illustrate the thick plate theory. The theoretical curves are based on the following simplifications:

(a) The medium is assumed to exert no shear stress in the central zone where faults can occur.

(b) The plastic energy per unit volume of armor in the path of the projectile is assumed to be constant through the thickness of the plate in the zone of irrotational flow, and is assumed to be the same as the energy in the equilibrium expansion of a hole of uniform diameter in the zone of equilibrium flow. The total plastic energy is assumed to be half the sum of the limiting energies for irrotational flow and equilibrium flow.

(c) The energy in the transverse undulation is assumed to be the same as the energy in an elastic undulation with the force concentrated at a point.

The theoretical and experimental curves are in excellent agreement. Curve II is included in Figure (9) to illustrate the limiting case of pure irrotational flow. Curve III is included to illustrate the limiting case of pure equilibrium flow. If there were no fault formation near the impact hole, the plate penetration coefficient should fall on Curve V.

VI EXPERIMENTAL FUNCTIONS

Ballistic data for 3" monobloc projectiles against homogeneous plate are summarized in Table I. A few supplementary data for bombs at low e/d are given in Table II, and the data for small caliber monobloc projectiles at high e/d are given in Tables III and IV. The data are based on non-deforming projectiles, except where noted in the tables. Impact parameters F_S were calculated from the original data for each impact and the plate penetration coefficients $F(e/d, \theta)$ were derived from the impact parameters with the aid of the penetration chart Figure (17) and the absorption chart Figure (18). The estimated values of the plate penetration coefficients for the actual conditions of impact are listed in the sixth column of the table. The probability is more than half, that the actual value of the plate penetration coefficient should fall within the range of uncertainty which has been assigned to each estimated value.

The plate penetration coefficient varies a small amount with the prevailing temperature of test. The effect of temperature on the plate penetration coefficient is not a linear function of temperature, but in a limited range of temperature the actual effect may be represented with sufficient accuracy by a linear relationship. At 15°C the plate penetration coefficient for a 3" monobloc projectile is lowered 4±1% per 100°C. increase in temperature. The limit energy function is lowered 8±2% per 100°C increase in temperature. Direct measurements at the Naval Research Laboratory on the change in hardness with temperature are also consistent with a decrease in tensile strength of 8±1% per 100°C rise in temperature. Equality between the temperature coefficients, for the limit energy function and for the tensile strength, is consistent with the theory for plates of constant ductility.

The plate penetration coefficient varies in a complicated manner, however, with the hardness of the plate. The effect of hardness was first investigated by the Naval Research Laboratory with cal. .30 AP bullets at a single value of e/d. The investigation has since been extended by the Naval Proving Ground and by the National Physical Laboratory to projectiles of larger caliber at other values of e/d. The plate penetration coefficient for a particular plate falls on a curve which rises with increase in hardness until a critical hardness is reached. Above the critical hardness the plate penetration coefficient drops to a lower curve. At a hardness less than the critical hardness the petals on the back of the plate remain intact, but above the critical hardness the plate failure is brittle. The critical hardness for brittle failure decreases with increase in projectile caliber, with decrease in plate thickness, and with increase in obliquity. The critical hardness is raised by an increase in carbon content, but is lowered by the presence of inhomogeneities in the steel. The critical hardness varies capriciously from plate to plate and from point to point in the same plate.

The effect of hardness on the plate penetration coefficient may be illustrated by a few extreme examples.

Plate penetration coefficients for 3" AP M79 projectiles against a series of ten 1"5 plates all from the same two heats are plotted against the tensile strengths of the plates in Figure (19). Two of the plates were investigated over a range of obliquity and the plate penetration coefficients for these plates are plotted against cosθ in Figure (20). Inspection of Figure (19) shows that the critical hardness for 30° obliquity occurred at a tensile strength of 115000±2000 (lb)/(in)^2. The plate penetration coefficients for Plate No. 40915 rose suddenly in Figure (20) as the obliquity was decreased from 14° to 8°, yet the plate penetration coefficients for Plate No. 40502 rose steadily with decrease in obliquity. The critical hardness was probably less than 123000 (lb)/(in)^2 for obliquities greater than 14°, but greater than 123000 (lb)/(in)^2 for obliquities less than 8°.

Plate penetration coefficients for 3" AP M79 projectiles against 2"5 CI Plates Nos. 87207 and 59533 are plotted against cosθ in Figure (21). Plate No. 87207 was received from the manufacturer with a tensile strength of 126000 (lb)/(in)^2. The plate threw large buttons on impact, and the plate penetration coefficients were low at both 0° and 30°. The buttons were flat cylinders, with smooth wiped faces and rough broken edges. Plate No. 87207 was retreated to a tensile strength of 112000 (lb)/(in)^2. After retreatment the plate failure was ductile and the plate penetration coefficients were higher, but still not as high as the plate penetration coefficients for Plate No. 59533. The brittle failure of Plate No. 87207 is believed to have been the result of segregations near the central plane. No flaws have been detected in this plate by the supersonic reflectoscope. Plate No. 59533 was heat treated to three different tensile strengths between 109000 (lb)/(in)^2 and 125000 (lb)/(in)^2. The plate failure was ductile, and the plate penetration coefficients increased with increase in tensile strength.

Plate penetration coefficients for 3" projectiles vs 1"2 CI Plate No. 55909 are plotted against cosθ in Figure (22). The tensile strength of the plate was 117000 $(lb)/(in)^2$. Two of the plate penetration coefficients at 0° were consistent with the results on other plates, but the rest of the plate penetration coefficients were very low. Two widely different limits were obtained at 0° with uncapped 3" AP Type A projectiles at different locations on the same plate.

The plate penetration coefficients for plates in the ductile range of hardness usually agree with each other to within a few percent. The effect of hardness on the plate penetration coefficient is not a linear function of hardness even in the ductile range of hardness, but in a limited range of hardness the actual effect may be represented with sufficient accuracy by a linear relationship. At a tensile strength of 115000 $(lb)/(in)^2$ the plate penetration coefficient is raised 0.3±0.1% per 1000 $(lb)/(in)^2$ increase in tensile strength. The limit energy function is increased 0.6±0.2% per 100 $(lb)/(in)^2$ increase in tensile strength. If the limit energy function were directly proportional to the static tensile strength, it would be raised 0.87% per 1000 $(lb)/(in)^2$ increase in tensile strength. The limit energy function is more likely to be proportional to the dynamic tensile strength. Measurements of the dynamic tensile strengths of various steels have been made by the California Institute of Technology. The data are summarized in Figure (23), where the dynamic tensile strength has been plotted against the static tensile strength. The ratio of dynamic tensile strength to static tensile strength is greatest for pure iron, and decreases to unity as the hardness increases. The general trend at a static tensile strength of 115000 $(lb)/(in)^2$ corresponds to an increase of dynamic tensile strength equal to 0.65±0.15% per 1000 $(lb)/(in)^2$ increase in static tensile strength. Attention is invited to the results for Class B armor and STS, which gave nearly the same dynamic tensile strengths for different static tensile strengths. The dynamic tensile strength of Class B armor is among the highest in Figure (23) for the same static tensile strength.

Any functions which are chosen to represent the basic relationships between the primary ballistic variables should be based on ductile armor, all at the same temperature, and all at the same static tensile strength. The mean annual temperature at Dahlgren is 15°C, so this was chosen as the standard temperature. A study of the ballistic data in 1944 suggested that 115000 $(lb)/(in)^2$ might be the maximum tensile strength at which the best quality of armor steel would remain ductile under all conditions of impact with 3" monobloc projectiles, so this was chosen as the standard tensile strength. The uncorrected plate penetration coefficients in the sixth column of Table I have been corrected to the standard temperature and standard tensile strength wherever there is sufficient internal evidence to form any basis for correction, and the corrected plate penetration coefficients are listed in the seventh column of the table. Many of the plates listed in the table had tensile strengths of 125000 $(lb)/(in)^2$, and may have had plate penetration coefficients either above or below the plate penetration coefficients for 115000 $(lb)/(in)^2$. Corrected and uncorrected plate penetration coefficients are both plotted in Figures (7) and (8).

The uncorrected plate penetration coefficients for small caliber monobloc projectiles in the sixth column of Tables III and IV have been corrected to the standard tensile strength, and also for scale and ogive. The corrected values are listed in the seventh column and are plotted in Figure (9).

Comparisons between the plate penetration coefficients for various projectile designs are obscured to a small extent by differences in the type of driving band or carrier. A jacket or plating on the nose of a projectile dart absorbs energy from the dart and raises the limit velocity, whereas a base cup or rotating band applies a force to the base of the dart and lowers the limit velocity. The plate penetration coefficient should be based on the mass of the dart with a fraction of the mass of the carrier added. The proper fraction to be added has never been determined, so the entire mass of the projectile is used in the calculations unless the major portion of the carrier obviously contributes nothing to the penetration. Thus the entire mass of the projectile has been used in the calculations for projectiles with plated or pressed driving bands, or base cups. Only the mass of the dart was used for projectiles with arrowheads, yet the arrowheads contributed a fraction of their kinetic energy to the energy of penetration. The plate penetration coefficients for arrowhead projectiles are therefore all low. A projectile with a sabot discards the sabot before impact, and the mass of the dart was therefore used for sabot projectiles.

The data for small caliber projectiles are consistent with the data for 3" projectiles except at the lowest value of e/d, where the small caliber projectiles have distinctly higher plate penetration coefficients. The formation of faults next to the impact hole may possibly occur with less frequency in the thinnest plates.

The choice of a continuous function to represent the limit energy function at any one obliquity should be governed by the data for all obliquities in order to reduce the effects of statistical fluctuations to a minimum. For values of e/d equal to or greater than 0.5 the limit energy function decreases consistently with increase in obliquity at a slightly greater rate than in direct proportion to $\cos\theta$. For values of e/d less than 0.5 the limit energy function for 3" AP M79 projectiles decreases with increase in obliquity more rapidly than at higher values of e/d, yet the limit energy function for 3" Comm Mk 3 projectiles against thin Mod STS actually increases with increase in obliquity. The noses of the common projectiles are flattened to a small extent on impact, however, and projectile deformation may be responsible for the increase in limit energy function with obliquity. In fact, the limit energy function for 3" common projectiles against thin mild steel decreases as it should with increase in obliquity and the projectiles are also undeformed. At least part of the variation in limit energy function with obliquity for thin plates is the result of changes in critical hardness. The various groups of data for low e/d are not consistent enough to justify the assumption of different obliquity effects for thin plate and thick plate.

The ballistic data at low obliquity are therefore summarized by a limit energy function $U(e/d,\theta)$ which is expressed analytically by the equation

$$U(e/d,\theta) = \left(\frac{e}{d}\right)\Phi^2\Theta\cos\theta \qquad (9)$$

in which Φ is the plate penetration coefficient for 0° obliquity, and Θ is a function of obliquity.

A master curve to represent the thickness function Φ is plotted in Figure (6), and is repeated as Curve I in Figures (1) to (22). The curve has been so adjusted by trial as to bring it into the best overall agreement with the ballistic data in the whole range of obliquity. Experimental values for the obliquity function Θ are listed in the ninth column of Table I and are plotted in Figures (11) to (16). The values of Θ were calculated with the values of $U(e/d,\theta)$ and Φ from the eighth column of Table I and from the master curve in Figure (6). The values of Θ in the figures are proportional to the limit energy per unit weight of armor in the path of the projectile. Curves are included in Figures (10) to (16), which probably best represent the obliquity function for ductile armor.

Table I (Continued)

Projectile	Plate Number	Plate Tensile Strength	θ	$\frac{e}{d}$	Uncorrect $F(\frac{e}{d}, \theta)$
3" AP M79	149824	128000	1.5°	.403	43000±20
"	"	124000	14°	.396	41900±20
"	"	128000	20°	.402	40100±30
"	"	128000	30°	.400	38500±20
"	"	124000	34°	.396	37800±20
"	"	128000	37.8°	.400	38000±20
"	158494	106000	0°	.0846	19300±50
"	167162	116000	.5°	1.373	48600±20
"	694385	130000	30°	.244	34200±20
"	F1790	115000	30°	.662	43900±20
"	F3076	85000	0°	.657	43700±20
"	"	85000	20°	.660	40000±20
"	"	85000	29.8°	.657	37900±20
"	"	85000	39.8°	.658	35000±20
"	"	85000	44.8°	.658	36400±20
"	X9021	120000	.5°	1.068	51600±40
"	X12904	122000	2°	.650	46500±30
"	"	122000	29.8°	.650	44700±30
"	X16835	132000	3°	.431	42800±50
"	"	132000	29.8°	.429	39600±30
"	X16919	130000	1°	.505	46100±30
"	"	130000	30°	.505	40700±20
"	X18305	110000	0°	.671	46300±30
"	"	110000	20°	.671	44500±20
"	"	110000	30°	.670	42600±20
"	"	110000	34.5°	.669	41700±20
"		110000	37°	.671	41500±20

UNCLASSIFIED

Table I (Continued)

late nsile ength	θ	$\frac{e}{d}$	Uncorrected $F(\frac{e}{d},\theta)$	Corrected $F(\frac{e}{d},\theta)$	$(10^{-8})\,U(\frac{e}{d},\theta)$	θ	cosθ
8000	1.5°	.403	43000±200		7.45	.991	1.000
4000	14°	.396	41900±200		6.95	.979	.970
8000	20°	.402	40100±300		6.46	.917	.940
8000	30°	.400	38500±200		5.93	.921	.866
4000	34°	.396	37800±200		5.66	.932	.829
8000	37.8°	.400	38000±200		5.78	.984	.790
06000	0°	.0846	19300±500	19800	.332	.795	1.000
16000	.5°	1.373	48600±200	48300	32.0	.893	1.000
30000	30°	.244	34200±200		2.85	1.042	.866
15000	30°	.662	43900±200	43900	12.77	1.016	.866
85000	0°	.657	43700±200	48500	15.46	1.074	1.000
85000	20°	.660	40000±200	44400	13.02	.958	.940
85000	29.8°	.657	37900±200	42100	11.65	.932	.868
85000	39.8°	.658	35000±200	38900	9.96	.900	.768
85000	44.8°	.658	36400±200	40400	10.73	1.050	.710
20000	.5°	1.068	51600±400	50600	27.4	1.049	1.000
22000	2°	.650	46500±300		14.05	.992	.999
22000	29.8°	.650	44700±300		12.99	1.056	.868
32000	3°	.431	42800±500		7.90	.951	.999
32000	29.8°	.429	39600±300		6.73	.940	.868
30000	1°	.505	46100±300		10.73	1.040	1.000
30000	30°	.505	40700±200		8.37	.936	.866
110000	0°	.671	46300±300	46800	14.70	.996	1.000
110000	20°	.671	44500±200	45000	13.60	.979	.940
110000	30°	.670	42600±200	43[illegible]	12.45	.975	.866
110000	34.5°	.669	41700±200	42[illegible]	11.86	.978	.824
110000	37°	.671	41500±200	4[illegible]	11.78	.999	.799

Table I (Continued)

Projectile	Plate Number	Plate Tensile Strength	θ	$\frac{e}{d}$	Uncorrected $F(\frac{e}{d},\theta)$	Cor F
3" AP M79	X18305	123000	.5°	.669	47000±200	4
"	"	123000	20°	.669	45200±300	4
"	"	123000	29.8°	.668	42800±200	4
"	X19797*	127000	1°	.513	41500±500	
"	"	127000	29.5°	.510	40200±500	
"	DD36	92000	.5°	1.443	48200±200	5
"	"	103000	.5°	1.403	49700±200	5
"	"	110000	.5°	1.440	51000±300	5
"	DD37	108000	0°	1.35	49100±200	5
"	"	108000	0°	1.39	49700±200	5
"	"	108000	15°	1.36	49500±200	5
"						
"	"	127000	0°	1.355	52900±500	5
"	"	135000	0°	1.355	54800±500	5
"	DD804	109000	30°	1.067	47500±200	4
"	GG125	116000	0°	1.61	52500±200	5
"	"	116000	0°	1.63	53000±500	5
"	GG296	97000	3°	.819	46100±200	4
"	"	97000	20°	.823	44400±300	4
"	"	97000	30°	.823	43700±500	4
"	"	103000	30°	.824	44000±500	4
"	"	111000	20°	.825	45700±100	4

*Laminated Plate

UNCLASSIFIED

Table I (Continued)

Plate Tensile Strength	θ	$\frac{e}{d}$	Uncorrected $F(\frac{e}{d},\theta)$	Corrected $F(\frac{e}{d},\theta)$	$(10^{-8})\,U(\frac{e}{d},\theta)$	θ	$\cos\theta$
123000	.5°	.669	47000±200	46600	14.52	.987	1.000
123000	20°	.669	45200±300	44800	13.43	.971	.940
123000	29.8°	.668	42800±200	42400	12.02	.942	.868
127000	1°	.513	41500±500		8.84	.839	1.000
127000	29.5°	.510	40200±500		8.25	.905	.870
92000	.5°	1.443	48200±200	51700	38.6	1.012	1.000
103000	.5°	1.403	49700±200	51300	36.9	1.004	1.000
110000	.5°	1.440	51000±300	51700	38.5	1.012	1.000
108000	0°	1.35	49100±200	50600	34.6	.988	1.000
108000	0°	1.39	49700±200	51300	36.6	1.008	1.000
108000	15°	1.36	49500±200	51000	35.4	1.035	.966
127000	0°	1.355	52900±500	50700	34.8	.992	1.000
135000	0°	1.355	54800±500	50800	35.0	.996	1.000
109000	30°	1.067	47500±200	48600	25.2	1.118	.866
116000	0°	1.61	52500±200	52500	44.4	1.011	1.000
116000	0°	1.63	53000±500	53000	45.8	1.027	1.000
97000	3°	.819	46100±200	48800	19.5	1.039	.999
97000	20°	.823	44400±300	47000	18.18	1.024	.940
97000	30°	.823	43700±500	46300	17.64	1.079	.866
103000	30°	.824	44000±500	45700	17.22	1.051	.866
111000	20°	.825	45700±100	46300	17.70	.994	.940

Table I (Continued

Projectile	Plate Number	Plate Tensile Strength	θ	$\frac{e}{d}$	Uncorre $F(\frac{e}{d},$
3" AP M79	GG346$\frac{1}{8}$	117000	.5°	1.035	50000
"	HH135	121000	0°	1.016	49400
"	"	121000	15°	1.020	48000
"	HH161	125000	1°	.975	49700
"	53E246A8	116000	30°	.662	42600

UNCLASSIFIED

tinued)

Table I (Continued)

ncorrect $F(\frac{e}{d},\theta)$	late ensile rength	θ	$\frac{e}{d}$	Uncorrected $F(\frac{e}{d},\theta)$	Corrected $F(\frac{e}{d},\theta)$	$(10^{-8})U(\frac{e}{d},\theta)$	Θ	$\cos\theta$
50000±50	17000	.5°	1.035	50000±500	49200	25.1	1.000	1.000
49400±50	21000	0°	1.016	49400±500	48700	24.1	.984	1.000
48000±20	21000	15°	1.020	48000±200	47400	22.9	.965	.966
49700±20	25000	1°	.975	49700±200	48200	22.7	.971	1.000
42600±10	16000	30°	.662	42600±1000	42400	11.92	.948	.866

Table I. Limit energy functions for 3" monobloc
ogival radius, vs STS of 115000 (lb)/(

Projectile	Plate Number	Plate Tensile Strength	θ	$\frac{e}{d}$	Uncorrec $F(\frac{e}{d}, \theta)$
3" Comm Mk 3	7404A	120000	2°	.083	21500±5
3" Comm Mk 3*	"	121000	30°	.085	23000±5
"	56360	123000	0°	.214	32100±2
"	"	"	4°	.209	31500±3
"	60919	122000	3°	.213	34500±3
"	"	"	4°	.217	35200±5
3" AP Type A**	"	"	10°	.212	34000±5
"	"	"	31°	.213	30500±5
3" Comm Mk 3	85830	127000	3°	.170	28500±1
3" AP Type A	"	127000	32°	.170	29500±1
3" Comm Mk 3	161855	118000	3°	.260	35800±2
3" AP Type A**	"	"	8°	.259	33800±2
3" AP Type A**	"	"	28.5°	.260	33500±5
3" Comm Mk 3	189679	109000	1°	.126	26300±
3" Comm Mk 3	624352	125000	3°	.203	35500±2
"	"	125000	6°	.205	35200±
"	B2680-CA7	145000	2°	.088	22500±
"	B2712-CA11	"	0°	.069	20500±
3" Comm Mk 3*	"	"	34°	.070	21500±

* Projectile with nose offset

** Uncapped projectile

BALLISTIC DATA

Limit energy functions for 3" monobloc projectiles with 1.67 caliber ogival radius, vs STS of 115000 (lb)/(in)^2 tensile strength, at 15°C.

Plate Tensile Strength	θ	$\frac{e}{d}$	Uncorrected $E(\frac{e}{d},\theta)$	Corrected $E(\frac{e}{d},\theta)$	$(10^{-8})U(\frac{e}{d},\theta)$	θ	$\cos\theta$
120000	2°	.083	21500±500		.428	.956	.999
121000	30°	.085	23000±500		.450	1.24	.866
123000	0°	.214	32100±200		2.21	.897	1.000
"	4°	.209	31500±300		2.07	.880	.998
122000	3°	.213	34500±300		2.54	1.038	.999
"	4°	.217	35200±500		2.69	1.063	.998
"	10°	.212	34000±500		2.45	1.028	.985
"	31°	.213	30500±500		1.98	.945	.857
127000	3°	.170	28500±1500		1.38	.887	.998
127000	32°	.170	29500±1000		1.48	1.118	.848
118000	3°	.260	35800±200		3.33	.932	.999
"	8°	.259	33800±200		2.96	.843	.990
"	28.5°	.260	33500±500		2.92	.928	.879
109000	1°	.126	26300±300		.885	1.000	1.000
125000	3°	.203	35500±200		2.56	1.150	.999
125000	6°	.205	35200±800		2.54	1.127	.994
145000	2°	.088	22500±300		.446	1.001	.999
"	0°	.069	20500±1000		.290	.972	1.000
"	34°	.070	21500±1000		.324	1.28	.829

Table I (Continued)

Projectile	Plate Number	Plate Tensile Strength	θ	$\frac{e}{d}$	Uncorrect $F(\frac{e}{d}, \theta)$
3" AP M79	1478	123000	30°	.655	43300±50
3" AP M79	9473	107000	.5°	1.68	51500±50
"	10359	91000	.5°	1.225	46200±40
"	"	92000	20°	1.300	45400±20
"	"	"	30°	1.298	43300±30
"	10650	104000	30°	.669	41500±20
"	40497	112000	29.7°	.489	41200±20
"	40498	127000	29.5°	.502	41500±20
"	40500	121000	29.8°	.488	41000±20
"	40502	104000	.5°	.495	43900±20
"	"	104000	20°	.495	42100±30
"	"	104000	30°	.490	40200±20
"	"	105000	38°	.488	37700±40
"	40819	117000	29.5°	.507	41300±20
"	40915	123000	1°	.493	46500±20
"	"	124000	8°	.502	46200±20
"	"	125000	14°	.490	43900±20
"	"	123000	20°	.495	42900±20
"	"	123000	29.7°	.498	41200±20
"	"	124000	40°	.497	39500±50
"	40916	113000	29.5°	.498	41300±20
"	40917	125000	29.5°	.494	41300±20

UNCLASSIFIED

Table I (Continued)

Plate Tensile Strength	θ	$\frac{e}{d}$	Uncorrected $F(\frac{e}{d}, \theta)$	Corrected $F(\frac{e}{d}, \theta)$	$(10^{-8})U(\frac{e}{d}, \theta)$	θ	cos θ
123000	30°	.655	43300±500		12.28	.988	.866
107000	.5°	1.68	51500±500	52600	46.5	1.000	1.000
91000	.5°	1.225	46200±400	50100	30.7	.992	1.000
92000	20°	1.300	45400±200	49100	31.4	.998	.940
"	30°	1.298	43300±300	46800	28.4	.985	.866
104000	30°	.669	41500±200	42800	12.25	.962	.866
112000	29.7°	.489	41200±200	41700	8.50	.988	.869
127000	29.5°	.502	41500±200				
121000	29.8°	.488	41000±200				
104000	.5°	.495	43900±200	45400	10.21	1.016	1.000
104000	20°	.495	42100±200	43500	9.37	.990	.940
104000	30°	.490	40200±200	41700	8.52	.992	.866
105000	38°	.488	37700±400	38900	7.39	.950	.788
117000	29.5°	.507	41300±200	41700	8.82	.978	.870
123000	1°	.493	46500±200	45200	10.07	1.009	1.000
124000	8°	.502	46200±200	44900	10.12	.997	.990
125000	14°	.490	43900±200	44200	9.57	.995	.970
123000	20°	.495	42900±200	43100	9.20	.972	.940
123000	29.7°	.498	41200±200	41800	8.70	.988	.869
124000	40°	.497	39500±500	39700	7.84	1.012	.766
113000	29.5°	.498	41300±200	41700	8.66	.983	.870
125000	29.5°	.494	41300±200				

Table I (Continued)

Projectile	Plate Number	Plate Tensile Strength	θ	$\frac{e}{d}$	Uncorrected $F(\frac{e}{d},\theta)$
3" AP M79	42024	102000	.5°	.368	41400±200
"	"	102000	20°	.370	39200±200
"	"	102000	30°	.368	37300±300
"	"	102000	37°	.371	35000±300
"	"	103000	41.5°	.369	34900±600
"	"	102000	44°	.370	34700±200
"	"	102000	49°	.372	36100±200
"	"	115000	0°	.367	43000±200
"	"	115000	19.8°	.370	41300±200
"	"	115000	30°	.368	37700±200
"	55909*	117000	2°	.408	43500±500
"	"	117000	31°	.435	35900±800
"	59533	109000	.5°	.809	48000±200
	"	109000	20°	.807	45500±200
"	"	109000	30°	.813	44800±600
"	"	113000	.5°	.813	48500±200
"	"	113000	20°	.808-	46600±200
"	"	113000	30°	.813	45300±300
"	"	115000	33°	.311	44500±300
"	"	125000	.5°	.813	48100±200
"	"	125000	19.5°	.812	47600±200
"	"	125000	24.3°	.813	46900±300
"	"	125000	28°	.812	45800±200
"	70015	110000	2°	.238	36300±200
"	"	109000	21°	.236	33300±200
"	"	109000	31°	.235	31100±200
"	"	112000	40°	.236	30200±200
"	"	109000	46.5°	.236	28800±100

*Brittle plate

UNCLASSIFIED

Table I (Continued)

Plate Tensile Strength	θ	$\frac{e}{d}$	Uncorrected $F(\frac{e}{d},\theta)$	Corrected $F(\frac{e}{d},\theta)$	$(10^{-8})\,U(\frac{e}{d},\theta)$	Θ	$\cos\theta$
1[illegible]000	.5°	.368	41400±200	43500	6.96	1.068	1.000
102000	20°	.370	39200±200	41100	6.25	1.009	.940
102000	30°	.368	37300±300	39100	5.63	.996	.866
102000	37°	.371	35000±300	36700	5.00	.944	.799
103000	41.5°	.369	34900±600	36600	4.95	1.004	.749
102000	44°	.370	34700±[illegible]	36400	4.90	1.035	.719
102000	49°	.372	36100±[illegible]	37900	5.34	1.227	.656
115000	0°	.367	43000±200	42800	6.72	1.033	1.000
115000	19.8°	.370	41300±200	41100	6.25	1.008	.941
115000	30°	.368	37700±200	37500	5.18	.916	.866
117000	2°	.408	43500±500	43200	7.61	.996	.999
117000	31°	.435	35900±800	35600	5.51	.764	.857
109000	.5°	.809	48000±200	48800	19.27	1.040	1.000
109000	20°	.807	45500±200	46200	17.23	.994	.940
109000	30°	.813	44800±600	45500	16.83	1.044	.866
11[illegible]000	.5°	.813	48500±200	48500	19.12	1.[illegible]27	1.000
11[illegible]000	20°	.808	46600±200	46700	17.62	1.015	.940
11[illegible]000	30°	.813	45300±300	45400	16.76	1.039	.866
11[illegible]000	35°	.811	44500±300	44400	16.00	1.026	.839
1[illegible]5000	.5°	.813	48100±200	47600	18.42	.989	1.000
125000	19.5°	.812	47600±200	47100	18.02	1.027	.943
135000	24.3°	.813	46900±300	46400	17.50	1.032	.911
125000	28°	.812	45800±200	45300	16.67	1.015	.883
110000	2°	.238	36300±200	36800	3.22	1.067	.999
109000	21°	.236	33300±200	33900	2.71	.973	.934
109000	31°	.235	31100±200	31700	2.36	.936	.857
112000	40°	.236	30200±200	30500	2.20	.961	.766
109000	46.5°	.236	28800±100	293[illegible]	2.03	.985	.688

Table I (Continued)

Projectile	Plate Number	Plate Tensile Strength	θ	$\frac{e}{d}$	Uncorrected $F(\frac{e}{d}, \theta)$	C
3" AP M79	70015	118000	.5°	.236	36900±200	
"	"	114000	20°	.236	34400±200	
"	"	118000	30°	.236	32600±200	
"	"	118000	38.2°	.236	30400±300	
"	"	118000	45°	.236	30100±200	
"	83880	122000	4°	.244	36900±200	
"	85187	87000	.5°	1.016	44300±200	
"	"	87000	30°	1.016	41200±200	
"	"	87000	35°	1.020	40900±200	
"	"	111000	.5°	1.021	48100±200	
"	"	111000	14°	1.020	48200±200	
"	"	110000	19.8°	1.024	46000±300	
"	"	126000	0°	1.007	50000±200	
"	"	126000	10°	1.002	48700±500	
"	"	126000	14.2°	1.005	48000±200	
"	87207*	112000	.5°	.806	46000±1000	
"	"	112000	30°	.806	44500±200	
"	"	126000	0°	.809	44500±500	
"	"	126000	30°	.809	43100±500	
"	87547	131000	1°	.650	47300±200	
"	"	131000	30°	.652	43800±500	
"	89002A	114000	.5°	.993	48200±200	4
"	89004A1	117000	.5°	.996	49400±200	4
"	89004A	116000	0°	.990	48600±400	4

*Brittle plate

UNCLASSIFIED

Table I (Continued)

late nsile rength	θ	$\frac{e}{d}$	Uncorrected $F(\frac{e}{d}, \theta)$	Corrected $F(\frac{e}{d}, \theta)$	$(10^{-8})\,U(\frac{e}{d}, \theta)$	θ	cosθ
18000	.5°	.236	36900±200	36400	3.13	1.045	1.000
24000	20°	.236	34400±200	34300	2.78	.987	.940
18000	30°	.236	32600±200	32100	2.43	.939	.866
18000	38.2°	.236	30400±300	30000	2.13	.903	.786
18000	45°	.236	30100±200	29700	2.08	.984	.707
22000	4°	.244	36900±200		3.32	1.053	.998
37000	.5°	1.016	44300±200	48900	24.3	.992	1.000
37000	30°	1.016	41200±200	45500	21.0	.992	.866
37000	35°	1.020	40900±200	45100	20.7	1.030	.819
11000	.5°	1.021	48100±200	48800	24.3	.988	1.000
11000	14°	1.020	48200±200	48900	24.4	1.022	.970
10000	19.8°	1.024	46000±300	46600	22.2	.953	.941
26000	0°	1.007	50000±200	48800	24.0	.992	1.000
26000	10°	1.002	48700±500	47500	22.6	.954	.985
26000	14.2°	1.005	48000±200	46800	22.0	.941	.969
12000	.5°	.806	46000±1000		17.05	.926	1.000
12000	30°	.806	44500±200		15.96	1.001	.866
26000	0°	.809	44500±500				
26000	30°	.809	43100±500				
31000	1°	.650	47300±200		14.55	1.026	1.000
31000	30°	.652	43800±500		12.52	1.016	.866
14000	.5°	.993	48200±200	48100	23.0	.964	1.000
17000	.5°	.996	49400±200	48900	23.8	.996	1.000
16000	0°	.990	48600±400	48200	23.0	.967	1.000

Table I (Continued)

Projectile	Plate Number	Plate Tensile Strength	θ	$\frac{e}{d}$	Uncorrected $F(\frac{e}{d}, \theta)$
3" AP M79	89001A7	114000	0°	1.010	49300±200
"	90940A1	91000	.5°	.664	45400±200
"	90940A	111000	.5°	.662	47300±500
"	90940A2	114000	0°	.665	47000±300
"	98193	116000	30°	.659	43200±200
"	107238	119000	2°	.455	45800±200
"	"	119000	30°	.455	40700±200
"	"	118000	35°	.460	39800±200
"	"	119000	45°	.460	41600±200
"	107716	120000	.5°	.666	46800±200
"	"	120000	20°	.668	44700±200
"	"	120000	29.8°	.668	42000±200
"	"	120000	34°	.666	41900±200
"	"	120000	40°	.660	42200±200
"	119652	117000	.5°	.326	40300±300
"	"	117000	30°	.326	34900±200
"	125687	118000	0°	.206	34300±200
"	"	118000	45°	.206	29200±500
"	127804A1	114000	.5°	1.010	48300±300
"	127804A2	114000	.5°	1.010	48500±200
"	140037	125000	0°	.202	34600±400
"	"	125000	20.2°	.204	32800±500
"	"	125000	30°	.204	31300±200
"	"	125000	40°	.204	29500±500
"	"	125000	45°	.203	30000±400

UNCLASSIFIED

Table I (Continued)

late sile ength	θ	$\frac{e}{d}$	Uncorrected $F(\frac{e}{d},\theta)$	Corrected $F(\frac{e}{d},\theta)$	$(10^{-8})U(\frac{e}{d},\theta)$	θ	$\cos\theta$
4000	0°	1.010	49300±200	49400	24.7	1.012	1.000
1000	.5°	.664	45400±200	47400	14.92	1.024	1.000
1000	.5°	.662	47300±500	47400	14.88	1.024	1.000
4000	0°	.665	47000±300	46900	14.62	1.002	1.000
6000	30°	.659	43200±200	43000	12.18	.975	.866
19000	2°	.455	45800±200		9.55	1.065	.999
19000	30°	.455	40700±200		7.54	.970	.866
18000	35°	.460	39800±200		7.29	.977	.819
19000	45°	.460	41600±200		7.96	1.239	.707
20000	.5°	.666	46800±200		14.60	1.000	1.000
20000	20°	.668	44700±200		13.35	.966	.940
20000	29.8°	.668	42000±200		11.78	.924	.868
20000	34°	.666	41900±200		11.70	.963	.829
20000	40°	.660	42200±200		11.76	1.061	.766
17000	.5°	.326	40300±300		5.29	.990	1.000
17000	30°	.326	34900±200		3.97	.857	.866
18000	0°	.206	34300±200		2.42	1.061	1.000
18000	45°	.206	29200±500		1.76	1.087	.707
14000	.5°	1.010	48300±300	48200	23.5	.964	1.000
14000	.5°	1.010	48500±200	48400	23.7	.972	1.000
25000	0°	.202	34600±400		24.2	1.099	1.000
25000	20.2°	.204	32800±500		21.9	1.047	.938
25000	30°	.204	31300±200		20.0	1.026	.866
25000	40°	.204	29500±500		17.76	1.030	.766
25000	45°	.203	30000±400		18.27	1.155	.707

Table II. Plate Penetration Coefficients for Bombs vs STS at low e/d

Bomb	Plate Number	θ	$\frac{e}{d}$	Uncorrected $F(\frac{e}{d},\theta)$	$(10^{-8})U(\frac{e}{d},\theta)$	θ	$\cos\theta$
Dm Bomb Mk 12	56360	44.5°	.046	19500±500	.175	1.4	.713
"	85830	20°	.036	≤ 16000			
"	131939	20°	.076	≤ 24800			
"	"	"	"	≥ 10500			
SAP Bomb T5	3A737A1	20°	.328	37000±1000	4.50	.9	.940
Dm Bomb Mk 12	Deck Target	15°	.071	19000±500	.256	.89	.966
"	"	18°	.054	22000±2000	.26	1.3	.951
Dm Bomb Mk 13	"	13°	.071	22000±1000	.34	1.1	.974
SAP Bomb T4	"	15.5°	.083	20000±2000	.33	.9	.964
"	"	16°	.089	27000±2000	.65	1.5	.961
"	"	16°	.133	28000±2000	1.04	1.1	.961
AP Bomb Mk 1	"	15°	.089	20000±2000	.36	.8	.966

Table III. Plate penetration coefficients at normal obliquity for geometrically similar scale model 2 pdr projectiles, based on the total mass of projectile with driving band included, and corrected for scale, ogive, and tensile strength to 3" scale, 1.67 cal. ogival radius, and 115000 $(lb)/(in)^2$ tensile strength.

Projectile Diameter	Plate Number	Brinell Hardness	$\frac{e}{d}$	Uncorrected $F(\frac{e}{d}, \theta)$	Corrected $F(\frac{e}{d}, \theta)$
.296"	2970	259	.757	53300	48900
"	2973	250	.977	54400	50600
"	2976	267	1.418	55800	50800
"	2980	257	1.831	57600	53000
.540"	2973	250	.536	53700	50400
"	2976	267	.777	52400	48200
"	2980	257	1.004	54000	50200
"	2986	255	1.501	54900	51200
"	2994	269	2.055	59400	54500
.990"	2980	257	.548	51600	48600
"	2986	255	.819	51400	48500
"	2994	269	1.121	54400	50500
"	3003	265	1.610	55400	51700
"	3011	258	2.139	58500	54900
1.565"	2994	269	.709	50000	46800
"	3003	265	1.019	51300	48200
"	3011	258	1.353	53900	51000
"	3021	259	2.013	55600	52600
1.565"	448	262	1.029	50800±300	48000
"	1467	266	1.534	55900±200	52100

Table IV. Plate penetration coefficients at normal obliquity for miscellaneous small caliber monobloc projectiles, corrected for scale, ogive, and tensile strength.

Projectile	d	Plate BHN	$\frac{e}{d}$	Uncorrected $F(\frac{e}{d},\theta)$	Corrected $F(\frac{e}{d},\theta)$
<u>Frankford Arsenal</u>					
cal .60 AP Dw 51	.588"	248	1.45	54000	52300
(miniature 3" AP M79)	"	255	1.52	56100	53800
<u>Naval Research Laboratory</u>					
cal .27 darts, bare	.2695"	266	.696	51300	48500
2.3 cal ogival radius	"	"	.928	52500	49800
	"	"	1.338	53500	50800
	"	"	1.855	54100	51700
<u>Princeton Range</u>					
cal .30 AP M2	.244"	294	1.045	49400	45800
in cal .50 arrowhead	"	264	2.44	52200	50500
	"	260	3.01	55200	53700
cal .30 AP M2, bare	.244"	262	1.87	53900	52300
Tungsten carbide projectile	.244"	260±10	2.06	58000±6000	54000
M-24-20 in cal .50 sabot	"	"	4.14	66000±4000	62000
1.25 cal ogival radius	"	"	6.15	67500±2000	63000
cal .50 AP E5, E6	.495"	294	.512	54800	48900
1.5 cal ogival radius	"	283	.751	55300	49000
	"	262	.97	52500	48700
	"	264	1.20	53000	49400
	"	272	1.98	56900	52800

Table IV. (continued)

Projectile	d	Plate BHN	$\frac{e}{d}$	Uncorrected $F(\frac{e}{d}, \theta)$	Corrected $F(\frac{e}{d}, \theta)$
20mm AP M-20mm-1	.786"	255	.98	49000	
20mm AP M-20mm-2	.786"	272	1.00	50000±5000	
1.5 cal ogival radius	"	307	1.90	53000±5000	
	"	260	3.20	62000±1000	58000
37mm AP Mk 1, Type 860	1.10"	266	5.40	65500±1000	62000

VIII

REFERENCES
(Ballistic Data)

1. "Penetration of Homogeneous Plate of One Tensile Strength (110,000 psi) by 3" M79 AP Projectiles. First Partial Report". US NPG Report No 8-44 (April, 1944)

2. "Penetration of Homogeneous Plate of one Tensile Strength (125,000 psi) by 3" M79 AP Projectiles. Second Partial Report". US NPG Report No 20-44 (July, 1944)

3. "Effect of Plate Tensile Strength on the Ballistic Limits of 2.0" Homogeneous Armor of Four Different Compositions against 37mm Capped AP, 3" M62 Capped AP, and 3" M79 Monobloc SAP projectiles. First Partial Report". US NPG Report No 9-45 (June, 1945)

4. "Armor penetration of cal. .60 Bullets of various contours" H. W. Euker and T. A. Read, Frankford Arsenal Report No R-615 (May 1945)

5. "The measurement of forces which resist penetration of STS armor, mild steel, and 24 ST aluminum". G. D. Kinzer, A. V. H. Masket, and J. R. Streeter, Naval Research Laboratory Report No. O-2276, (April, 1944)

6. "The Ballistic Properties of Mild Steel", NDRC Report No. A-111, (November, 1942); "Ballistic Tests of STS Armor Plate, using 37mm Projectiles" NDRC Report No. A-156, (March, 1943)

7. "High velocity terminal ballistic performance of cal. .30 AP M2 steel cores" R. J. Emrich and C. W. Curtis, NDRC Report No. A-282 (July, 1944)

8. "Capped projectiles at hypervelocities" R. J. Emrich, NDRC Monthly Report No. OTB-1 (August 15, 1944); "Comparison of capped and monobloc steel projectiles at hypervelocities", R. J. Emrich, J. R. Sproule, C. W. Curtis, NDRC Monthly Report No. OTB-3 (October 15, 1944); "Subcaliber steel projectiles" C. W. Curtis and R. J. Emrich, NDRC Monthly Report No. OTB-8d (March 15, 1945); "Effect of armor piercing cap on perforation limits", C. W. Curtis and J. R. Emrich NDRC Monthly Report OTB-10g (May 15, 1945)

9. "Terminal ballistics of tungsten carbide projectiles, survey and nose-shape tests". C. W. Curtis, R. J. Emrich, J. R. Sproule, NDRC Monthly Report No OTB-7 (February 15, 1945); "Terminal ballistics of tungsten carbide projectiles. Effect of carrier Part I". E. R. Jones, C. W. Curtis, R. J. Emrich NDRC Monthly Report No. OTB-12a (July 15, 1945)

10. "The effect of the shape of the head of AP shot on critical velocities for penetration at normal". M. R. MacPhail, Proof and Development Establishment, Valcartier, P. Q. Canada (May, 1943); "Second progress report on the investigation of scale effect in armour penetration. Effect of hardness on plate performance". D. C. Sopwith, A. F. C. Brown, and V. M. Hickson, National Physical Laboratory Report No. 50 (February, 1943); "Third progress report on the investigation of scale effect in armour penetration. Firing trials at normal attack with geometrically similar shot against homogeneous armour of varied hardness". A. F. C. Brown and V. M. Hickson, National Physical Laboratory Report No. 79 (September, 1944)

NPG PHOTO NO. 2971 (APL)

COMPARISON OF PLATE PENETRATION COEFFICIENTS

FIGURE (1)

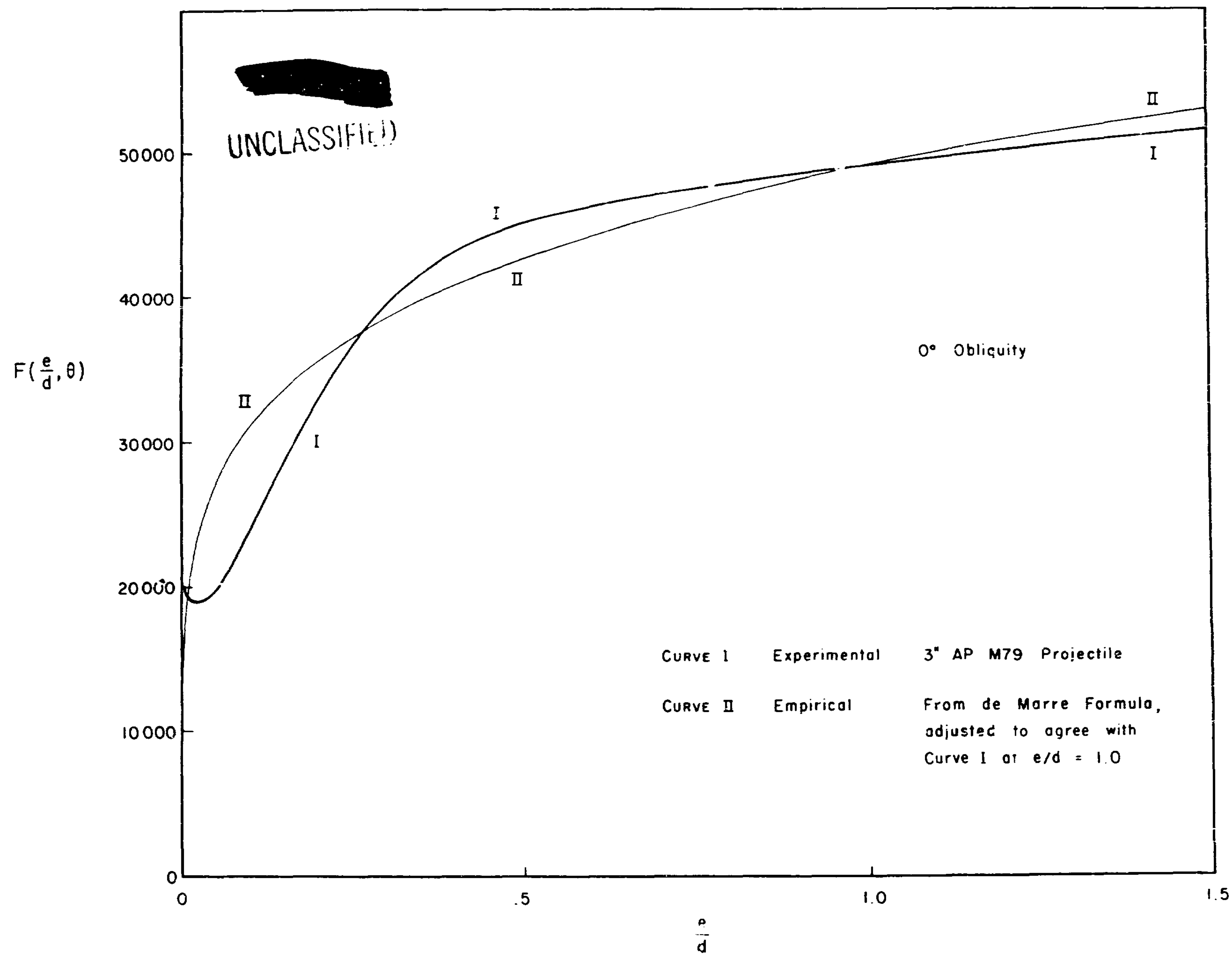

NPG PHOTO NO. 2972 (APL)

COMPARISON OF PLATE PENETRATION COEFFICIENTS

FIGURE (2)

[redacted]

UNCLASSIFIED

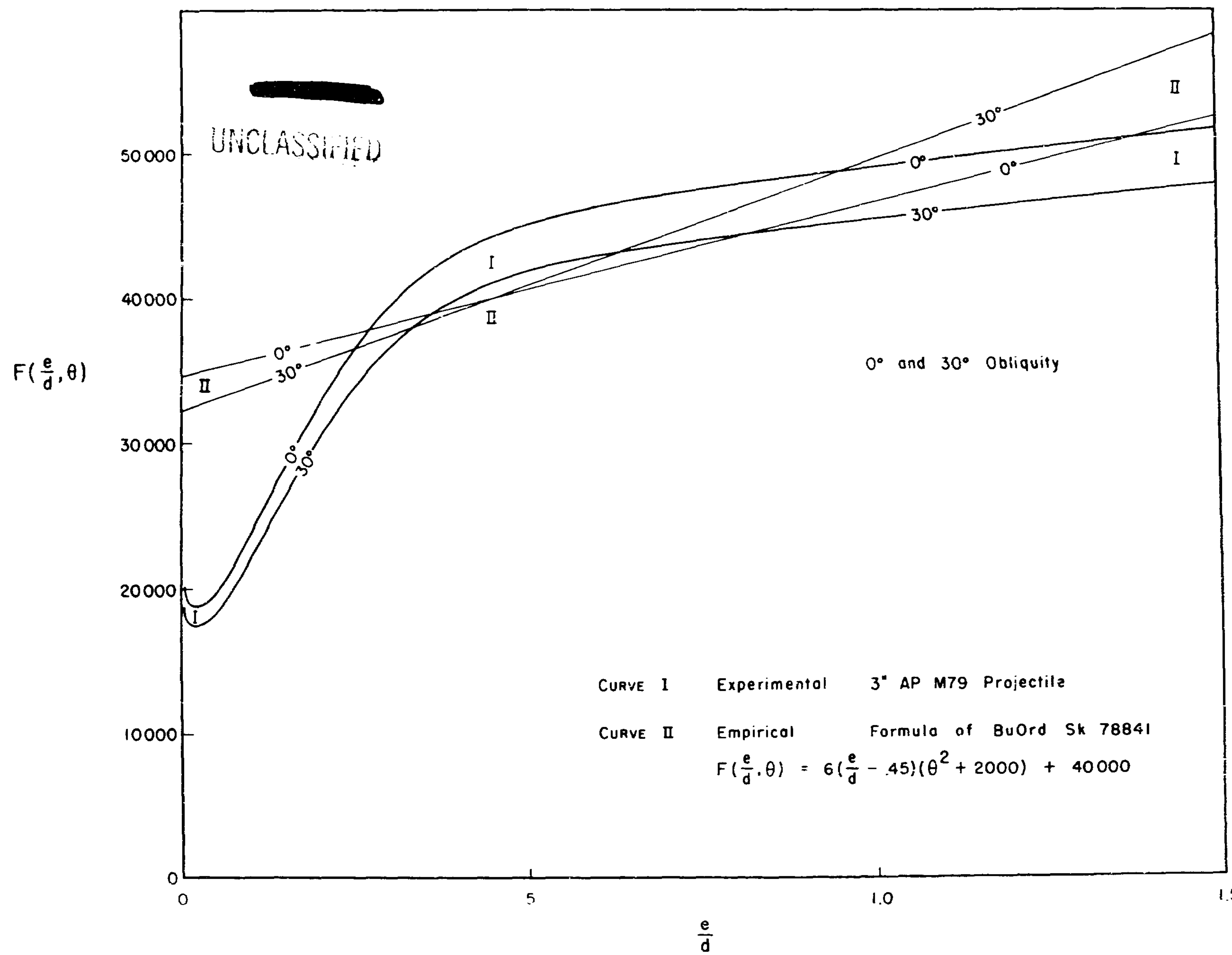

NPG PHOTO NO. 2973 (APL)

COMPARISON OF PLATE PENETRATION COEFFICIENTS

FIGURE (3)

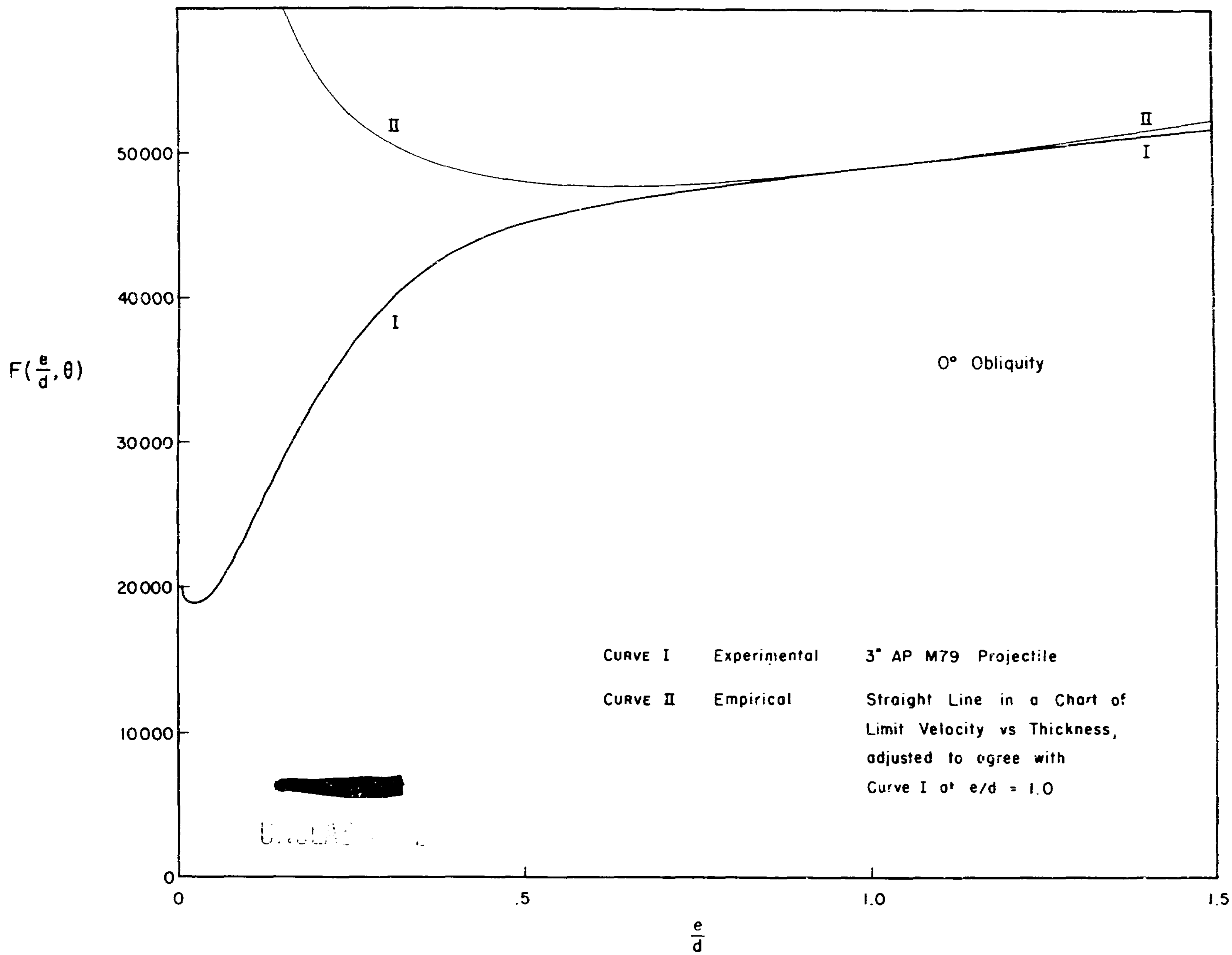

NPG PHOTO NO 2974 (APL)

COMPARISON OF PLATE PENETRATION COEFFICIENTS

FIGURE (4)

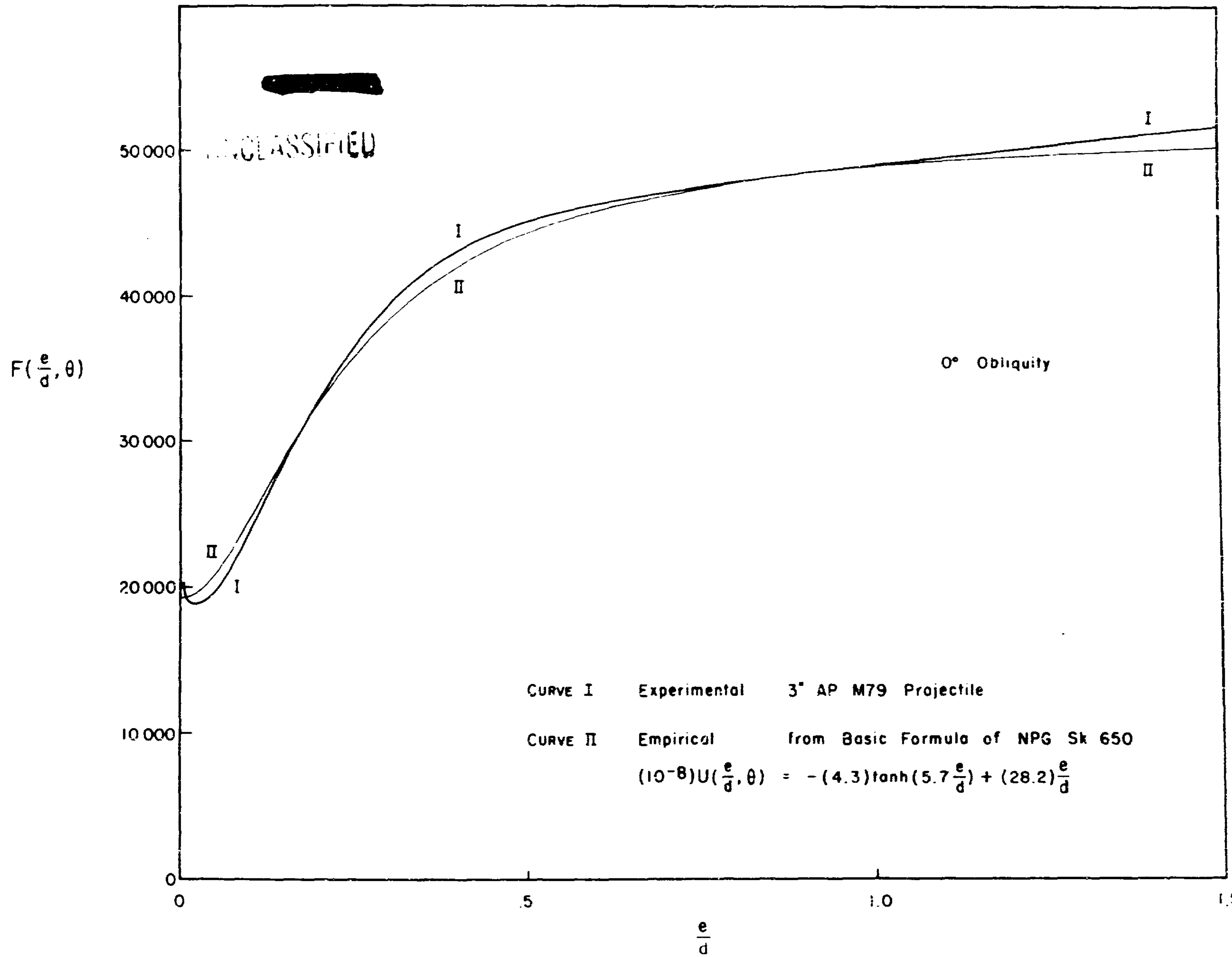

NPG PHOTO NO 2975 (APL)

COMPARISON OF PLATE PENETRATION COEFFICIENTS

FIGURE (5)

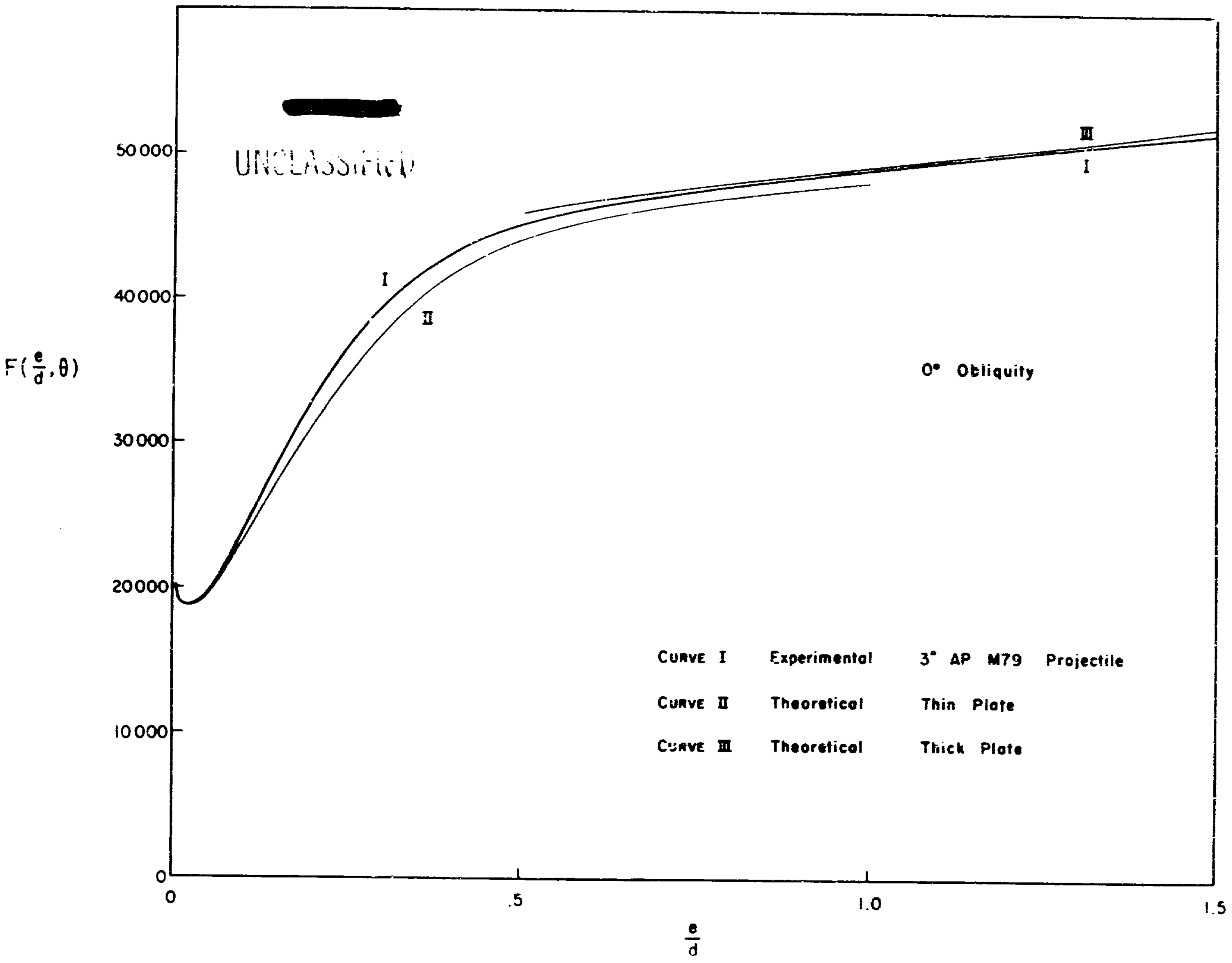

NPG PHOTO NO. 2976 (APL)

[redacted] UNCLASSIFIED

FIGURE (6)

THE PLATE PENETRATION COEFFICIENT FOR 0° OBLIQUITY

Standard Experimental Curve for 3" AP M79 Projectile vs STS of 115000 (lb)/(in)^2 Tensile Strength at 15°C

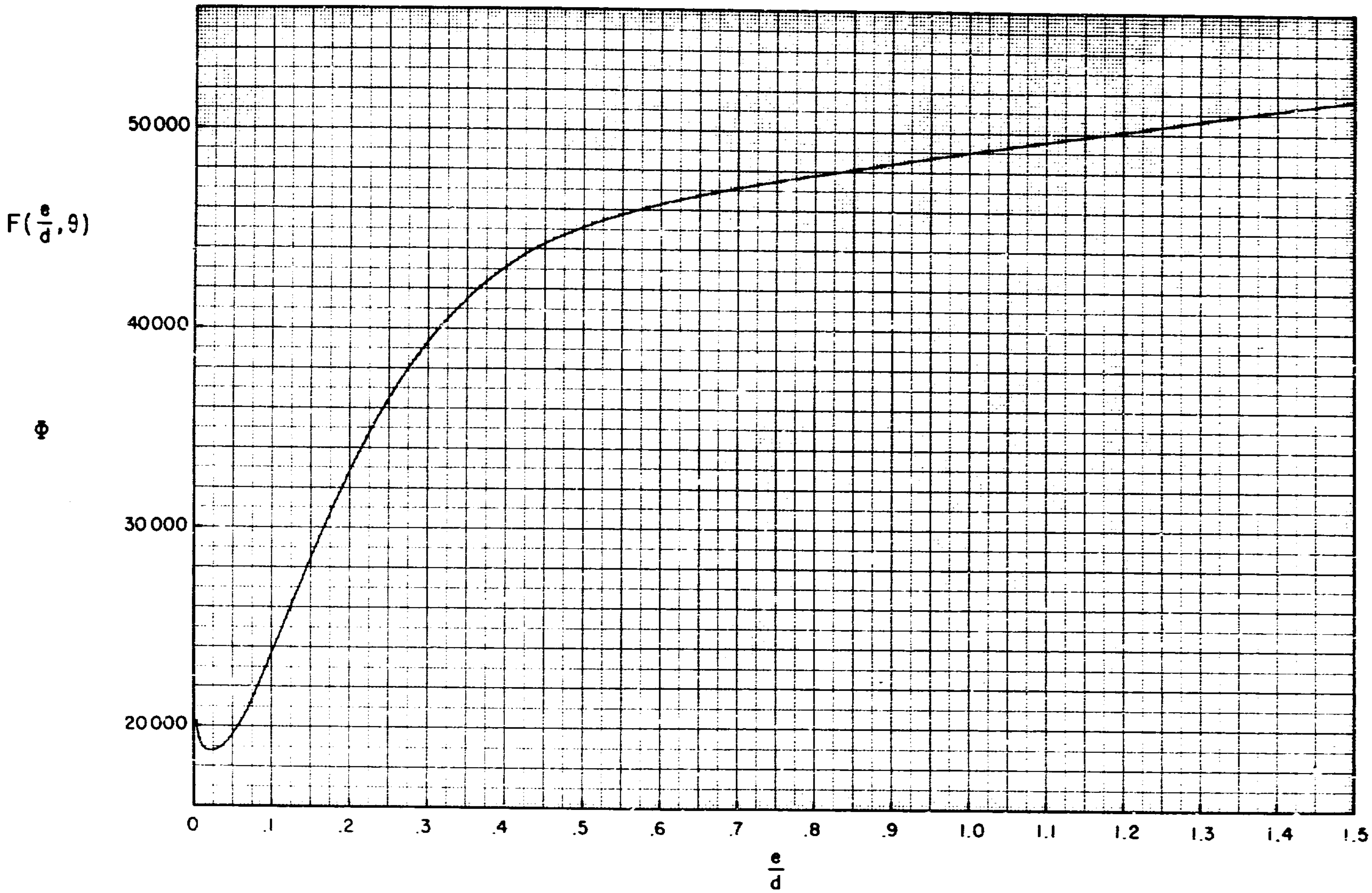

NP 4OTO NO. 2977 (APL) FIGURE (7)

PLATE PENETRATION CO FICIENTS

Undeformed 3" Monobloc Projectiles vs STS at 0° Obliquity, corrected to 115000 (lb)/(in)^2 Tensile Strength and 15°C

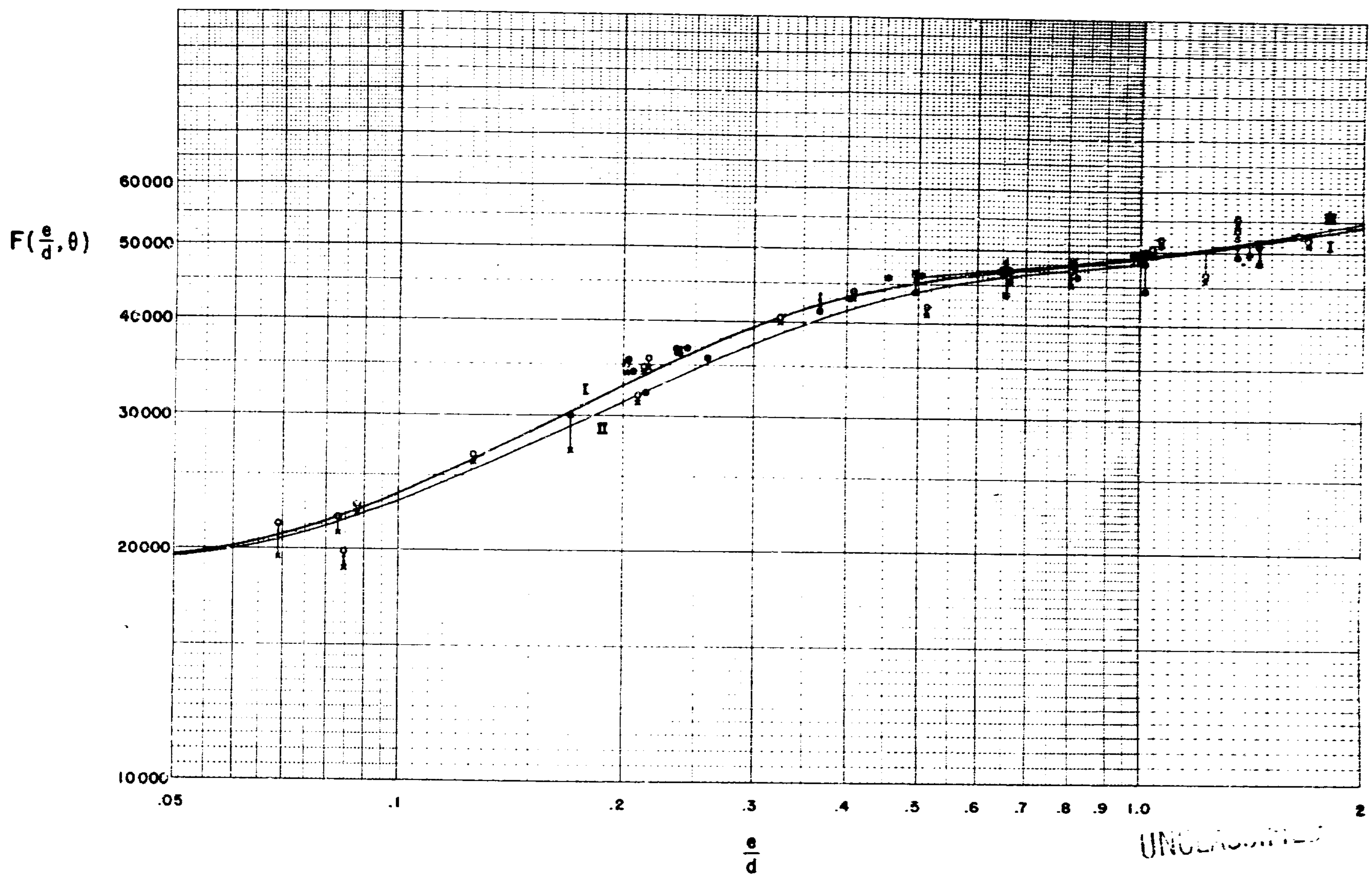

UNCL

[redacted]

- ○ Complete Penetration, estimated minimum value
- x Incomplete Penetration, estimated maximum value
- ● Limit Determination, uncorrected
- • Limit Determination, corrected

CURVE I	Standard	3" AP M79 Projectile
CURVE II	Theoretical	Thin Plate
CURVE III	Theoretical	Thick Plate

NPG PHOTO NO. 2978 (APL)

PLATE PENETRATION COEFFICIENTS

FIGURE (9)

Undeformed 3" Monobloc Projectiles vs STS at 30° Obliquity, corrected to 115000 (lb)/(in)^2 Tensile Strength and 15°C

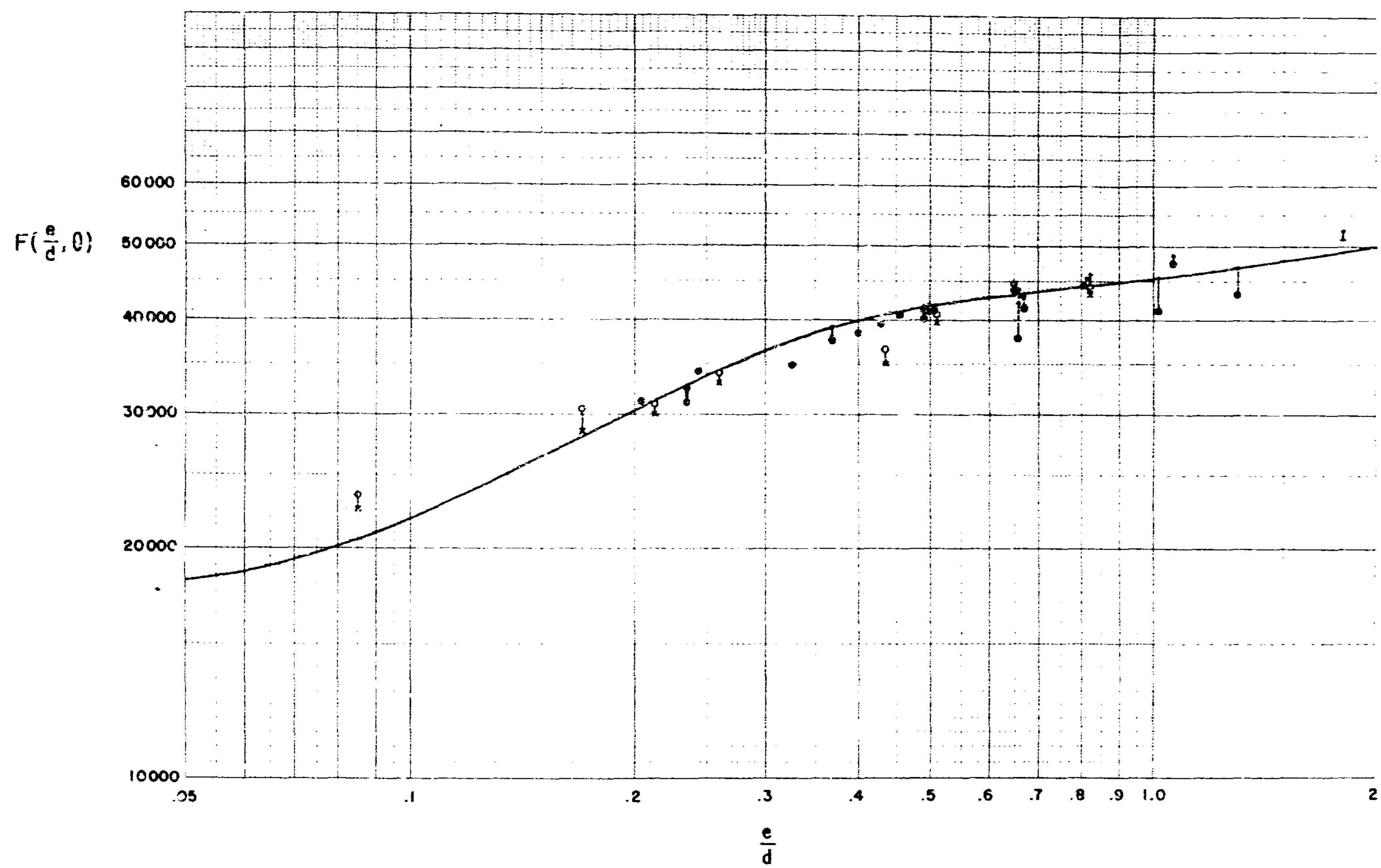

Complete Penetration, estimated minimum value

Incomplete Penetration, estimated maximum value

Limit Determination, uncorrected

Limit Determination, corrected

CURVE I Standard 3" AP M79 Projectile

NPG PHOTO NO. 2979 (APL) | FIGURE (9)

PLATE PENETRATION COEFFICIENTS

Small Caliber Monobloc Projectiles vs Homogeneous Plate at 0° Obliquity, corrected for Scale, Ogive, and Tensile Strength, to 3" Scale, 1.67 Caliber Ogival Radius, and 115000 (lb)/(in)^2 Tensile Strength

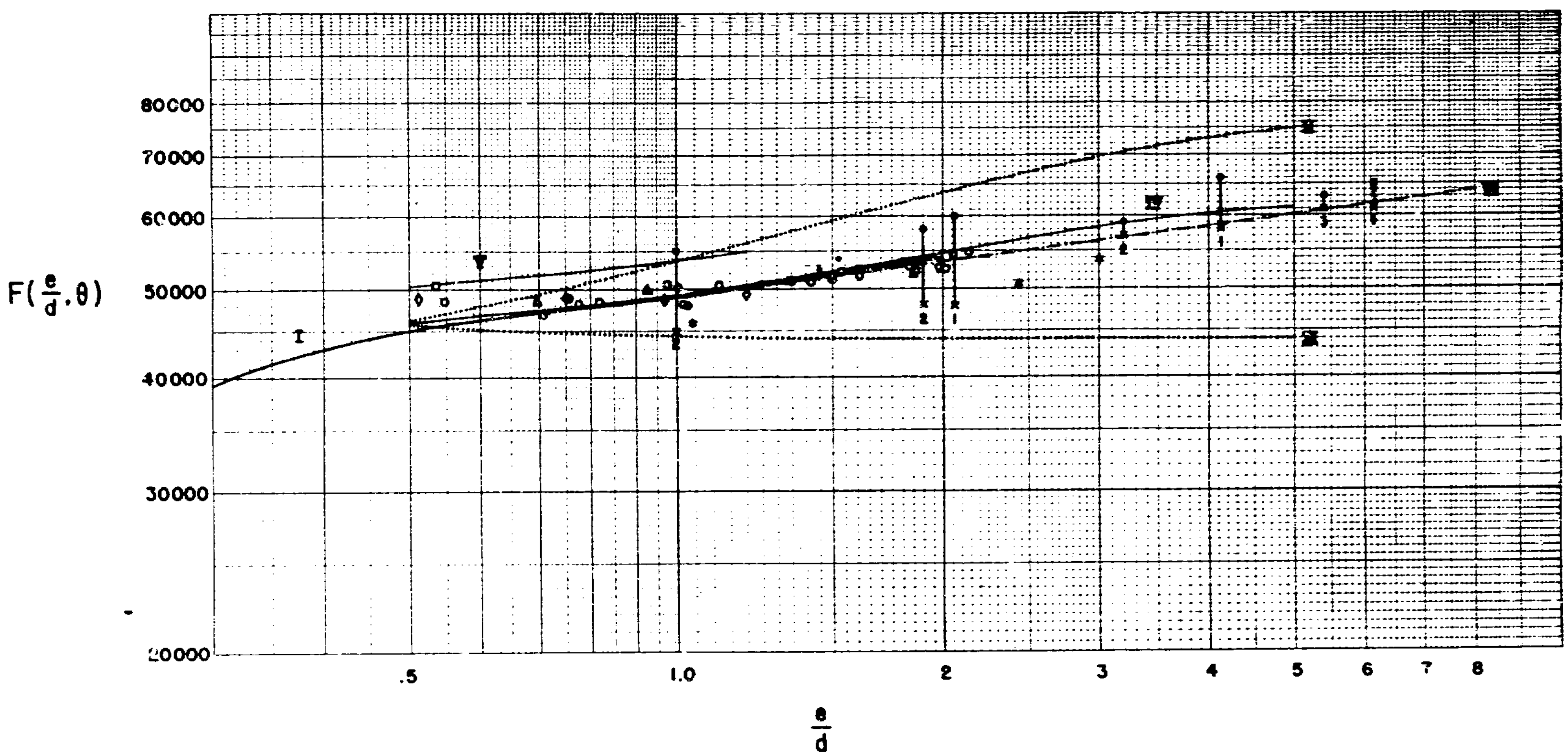

SYMBOL	CALIBER	TYPE	OGIVAL RADIUS	CARRIER
o	".303 to 40mm	2 pdr models	1.4 Cal	Plating or Band
•	".60	FA Dw 51	1.67 Cal	Base Cup
Δ	".27	Steel Dart	2.5 Cal	None
□	".30	AP M2 Dart	3 Cal	None
*	".30	AP M2 Dart	3 Cal	Cal .50 Arrowhead
x 1	".30	M-24-20	1.25 Cal	Cal .50 Sabot
◊	".50	E5, E6	1.5 Cal	Rotating Band
x 2	20mm	M-20mm-2	1.5 Cal	Base Cup or Sabot
x 3	".10	Mk I, Type 860	1.4 Cal + 80° Cone	Sheath and Sabot

CURVE I	Experimental	3" AP M79 Projectile
CURVE II	Theoretical	Irrotational Flow with Fault Formation
CURVE III	"	Equilibrium Flow with Fault Formation
CURVE IV	"	Thick Plate with Fault Formation
CURVE V	"	Thick Plate without Fault Formation
CURVE VI	Empirical	from Princeton Station Formula

$$(10^{-8})U(\frac{e}{d},\theta) = 24(\frac{e}{d})^{1.26}$$

UNCLASSIFIED

NPG PHOTO NO. 2980 (APL) FIGURE (10)

COMPARISON OF OBLIQUITY FUNCTIONS

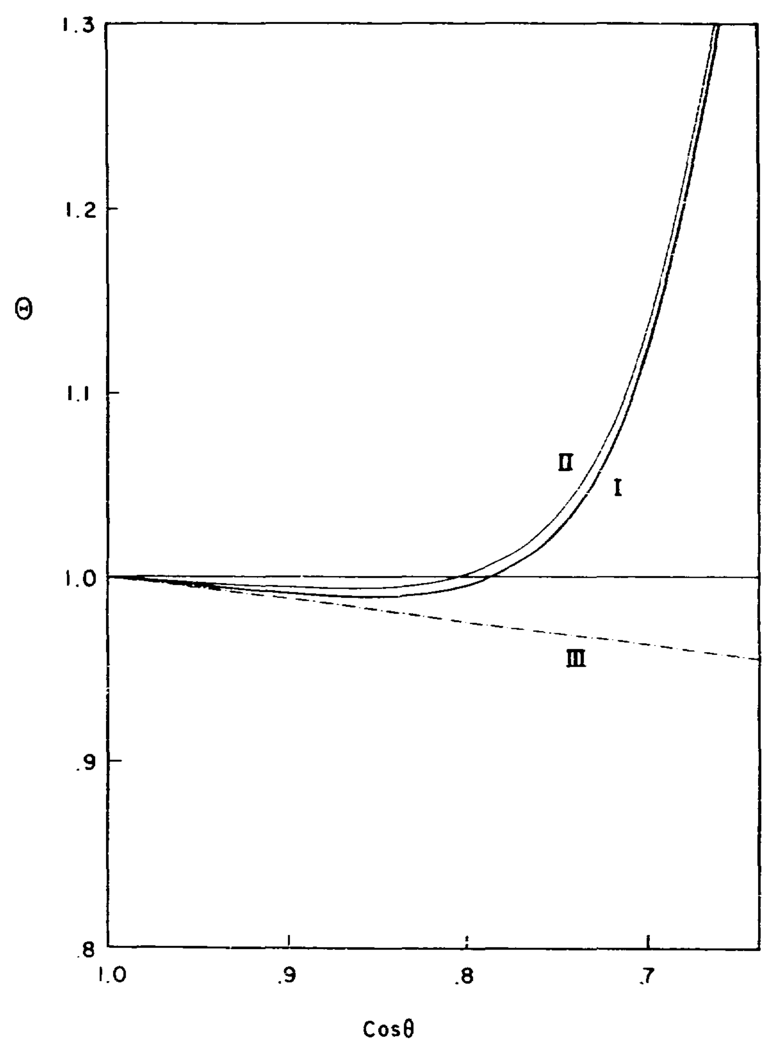

CURVE I Experimental
3" AP M79 Projectile

CURVE II Empirical
Basic Formula of NPG Sk 650

$$\theta = 1 + \frac{5}{\sqrt{\pi}}\int_{-\infty}^{6.6\left(\frac{1}{2} - \cos\theta\right)} e^{-\beta^2}\,d\beta - .03\sin^2\theta$$

CURVE III Theoretical
Thick Plate without Ricochet

UNCLASSIFIED

[redacted]

NPG PHOTO NO. 2981 (APL)

[redacted]

FIGURE (11)

OBLIQUITY FUNCTIONS FOR e/d < .5

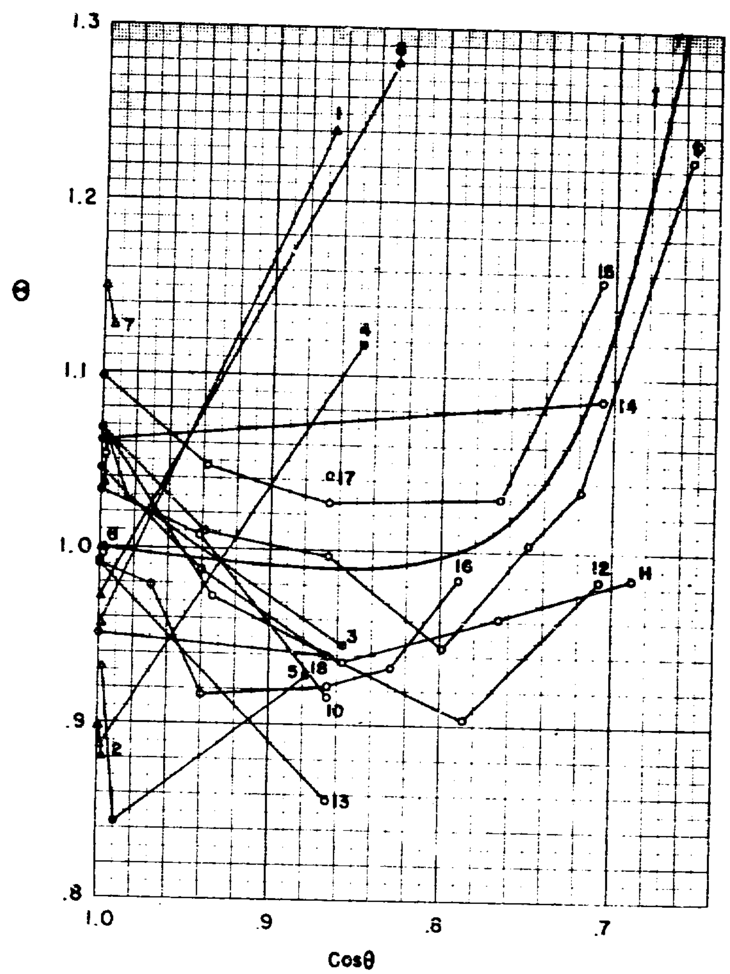

Symbol	Projectile
Δ	3" Comm Mk 3
●	3" AP Type A uncapped
○	3" AP M79

Key	Plate	Tensile Strength
1	7404A	120000
2	56360	123000
3	60919	122000
4	85830	127000
5	161855	118000
6	189679	109000
7	624352	125000
8	82712-CAII	145000
9	42024	102000*
10	42024	115000*
11	70015	110000*
12	70015	118000*
13	119652	117000
14	125687	118000
15	140037	125000
16	149824	128000
17	694385	130000
18	X16835	132000

*Obliquity functions corrected for tensile strength to 115000

NPG PHOTO NO 2982 (APL) FIGURE (12)

OBLIQUITY FUNCTIONS FOR 3" AP M79 PROJECTILE AT e/d = .5

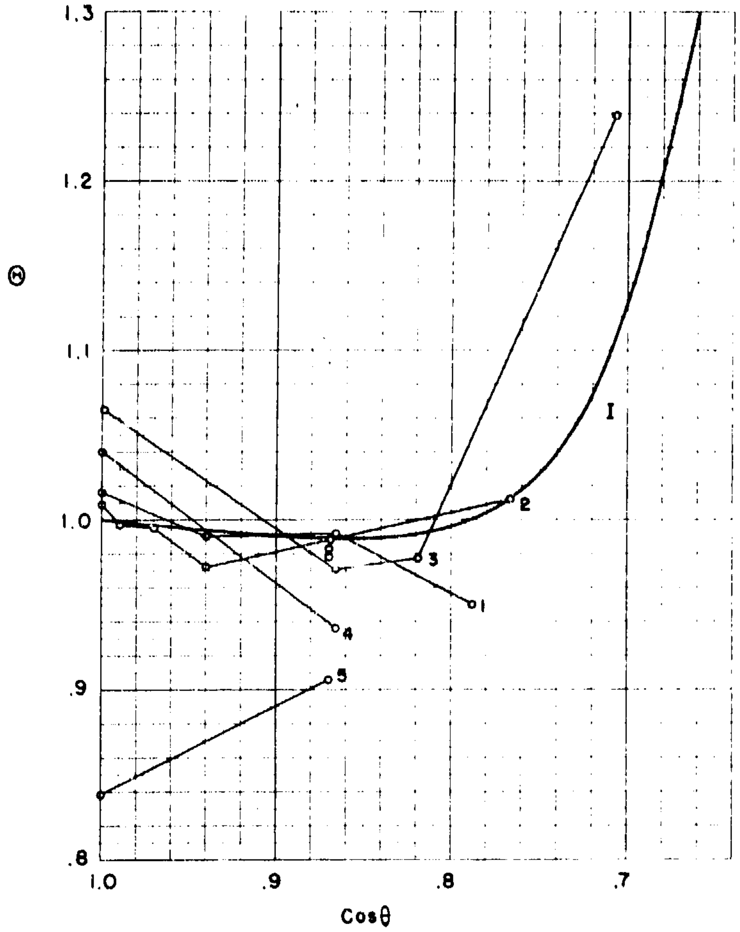

KEY	PLATE	TENSILE STRENGTH
1	40502	104000*
2	40915	123000*
3	107238	119000
4	X16919	130000
5	X19797	127000

*Obliquity functions corrected for tensile strength to 115000

CURVE I Standard

UNCLA

[redacted]

OBLIQUITY FUNCTIONS FOR 3" AP M79 PROJECTILE AT e/d = .65

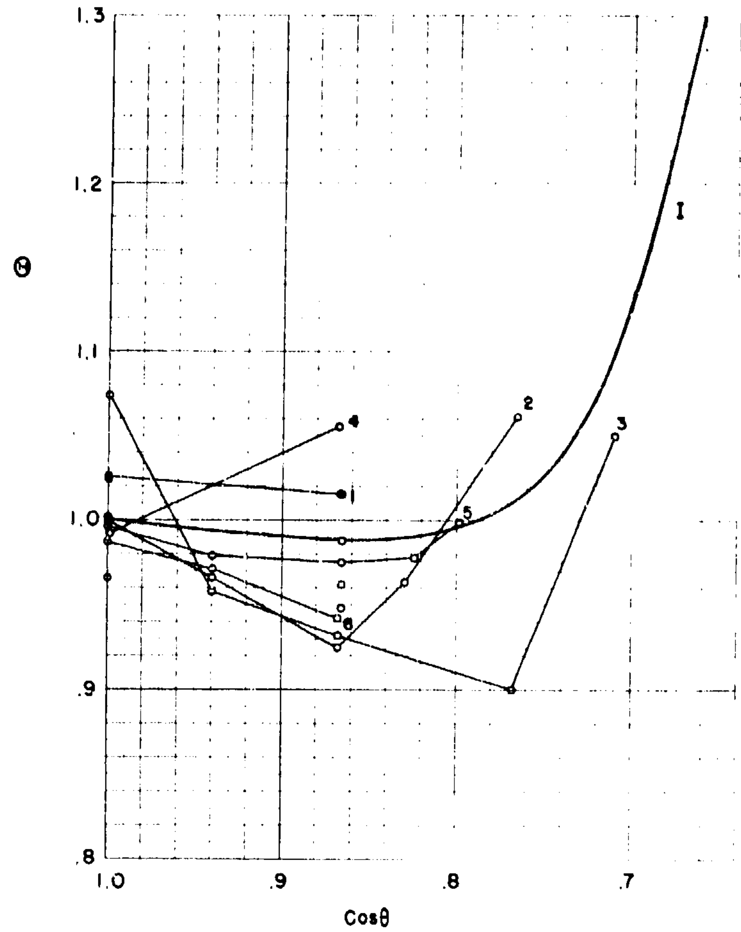

KEY	PLATE	TENSILE STRENGTH
1	87547	130000
2	107716	120000
3	F3076	85000*
4	X12904	122000
5	X18305	110000*
6	X18305	123000*

*Obliquity functions corrected for tensile strength to 115000

CURVE I Standard

[redacted]

NPG PHOTO NO. 2984 (APL) FIGURE (14)

OBLIQUITY FUNCTIONS FOR 3" AP M79 PROJECTILE AT e/d = .82

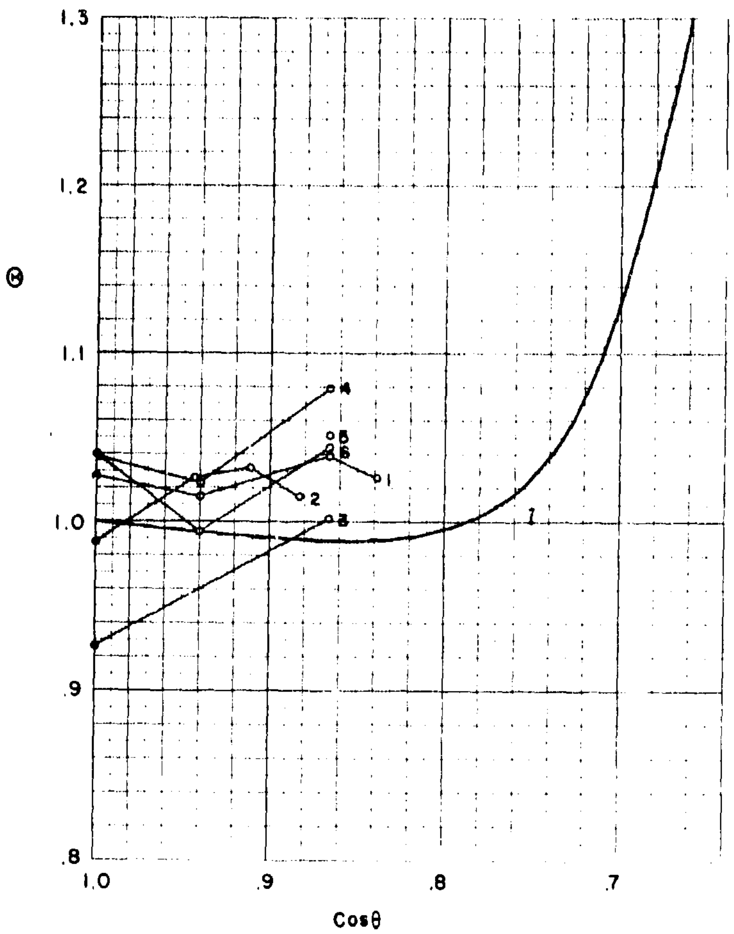

Key	Plate	Tensile Strength
1	59533	115000*
2	59533	125000*
3	87207	112000
4	GG296	97000*
5	GG296	103000*
6	GG296	111000*

*Obliquity functions corrected for tensile strength to 115000

Curve I Standard

UNCLASSIFIED

[redacted]

NPG PHOTO NO. 2985 (APL)

FIGURE (15)

OBLIQUITY FUNCTIONS FOR 3" AP M79 PROJECTILE AT e/d = 1.0

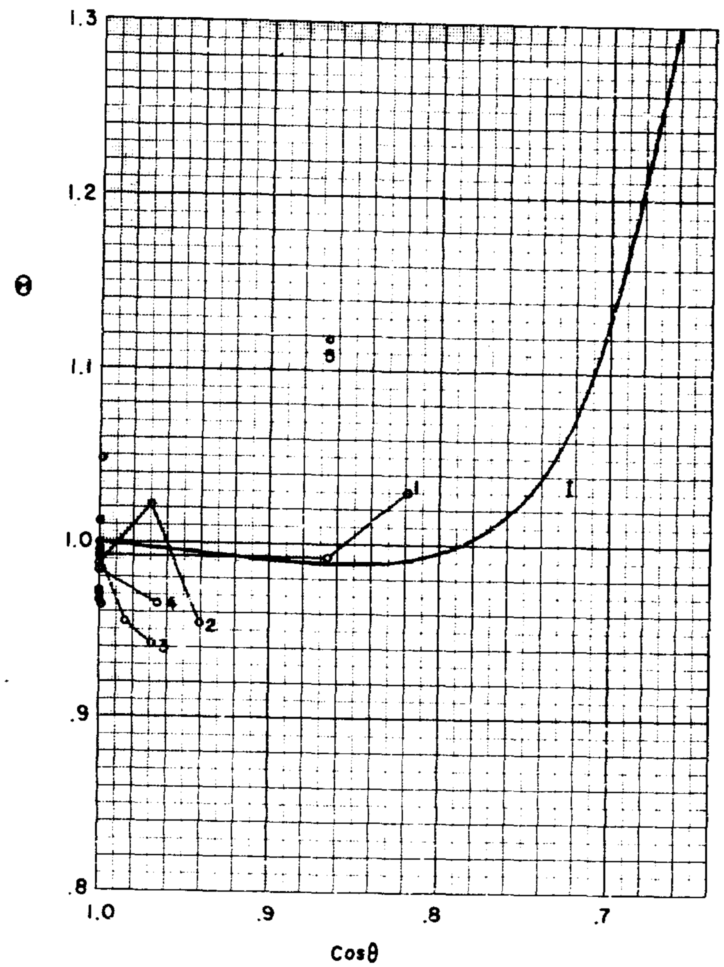

KEY	PLATE	TENSILE STRENGTH
1	85187	87000*
2	85187	110000*
3	85187	126000*
4	HH'35	121000*
5	DD804	109000*

*Obliquity functions corrected for tensile strength to 115000

CURVE I Standard

CLASSIFIED

[redacted]

NPG PHOTO NO. 2986 (APL)

FIGURE (16)

OBLIQUITY FUNCTIONS FOR 3" AP M79 PROJECTILE AT e/d > 1.0

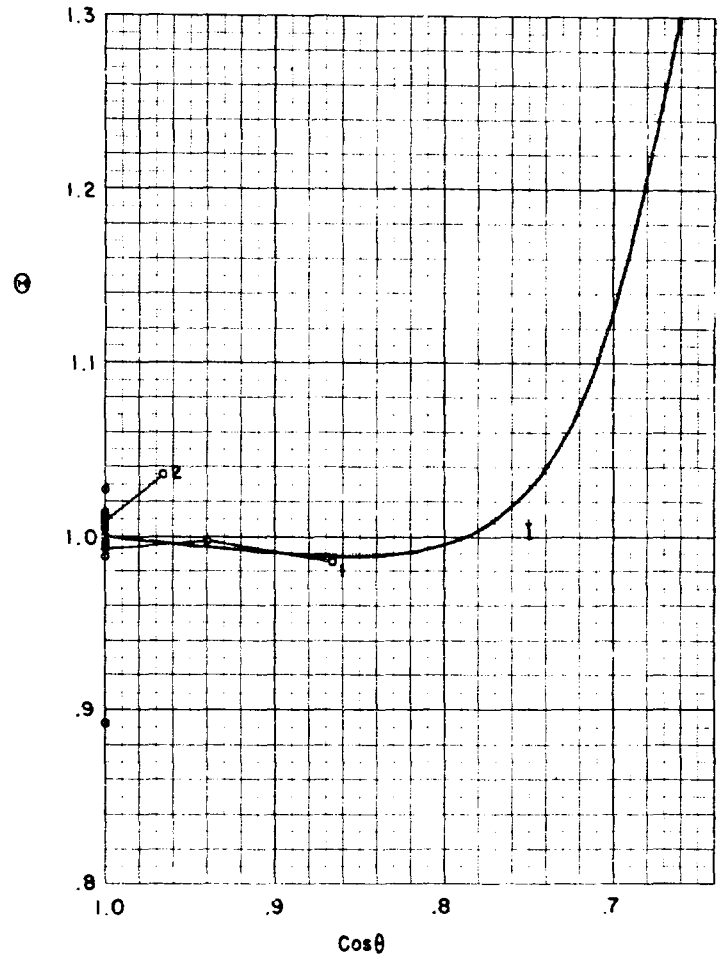

Key	Plate	Tensile Strength
1	10359	92000*
2	DD37	108000*

*Obliquity functions corrected for tensile strength to 115000

Curve 1 Standard

UNCLASSI...

[redacted]

NPG PHOTO NO. 2987 (APL) FIGURE (17)

THE DEPTH OF PENETRATION

3" AP M79 Projectile in Homogeneous Plate at Low Obliquity

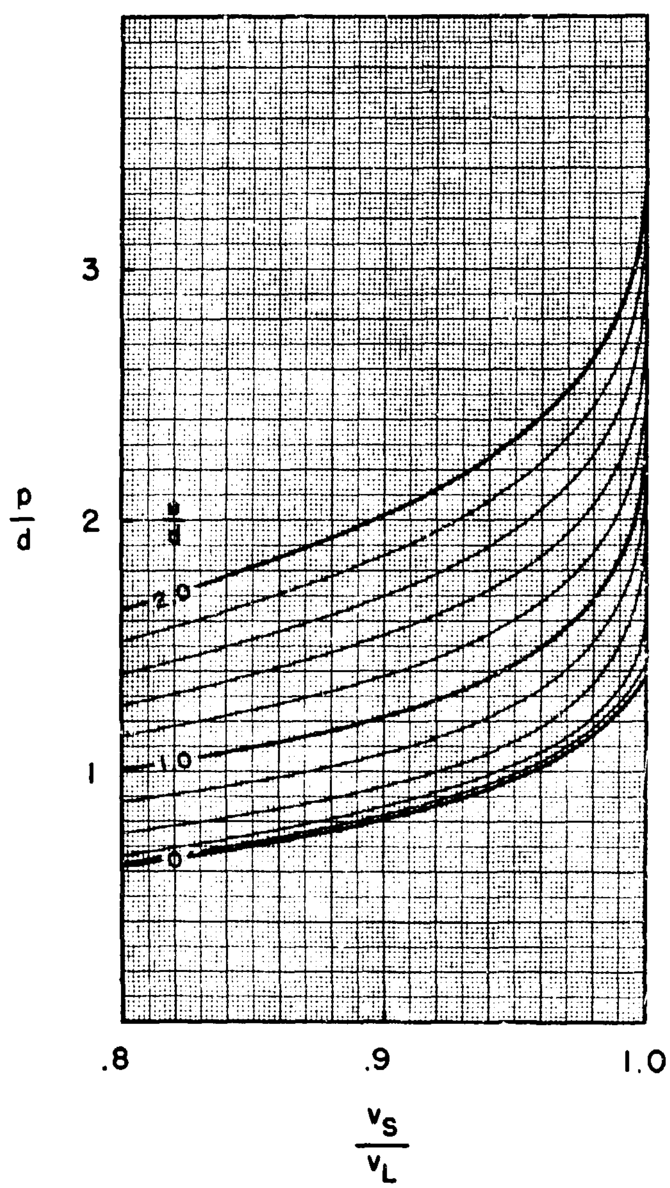

e = plate thickness

d = projectile diameter

p = depth of penetration

v_S = striking velocity

v_L = limit velocity

UNCLASSIFIED

[redacted]

NPG PHOTO NO 2988 (APL)

ABSORPTION JNCTIONS

FIGURE (1d)

3" AP M79 Projectile in Homogeneous Plate at 0° Obliquity

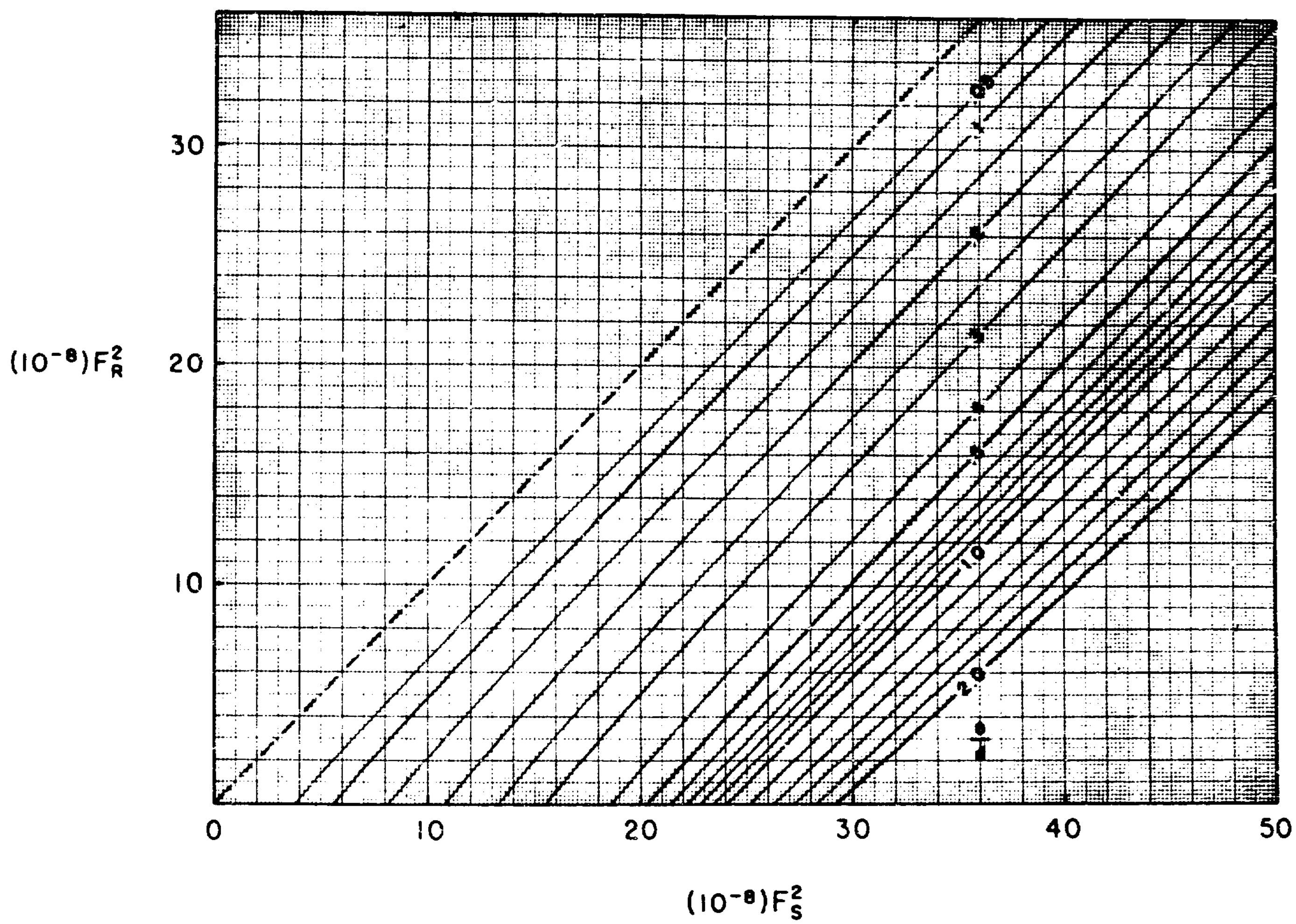

m = projectile mass (lb)

d = projectile diameter (ft)

e = plate thickness (ft)

θ = obliquity

v_S = striking velocity (ft)/(sec)

v_R = remaining velocity (ft)/(sec)

[redacted]

$$F_S^2 = \frac{mv_S^2\cos^2\theta}{ed^2}$$

$$F_R^2 = \frac{mv_R^2\cos^2\theta}{ed^2}$$

NPG PHOTO NO 2989 (APL) [redacted] FIGURE (19)

PLATE PENETRATION COEFFICIENTS

3" AP M79 Projectile vs Ten Plates of STS from Two Heats

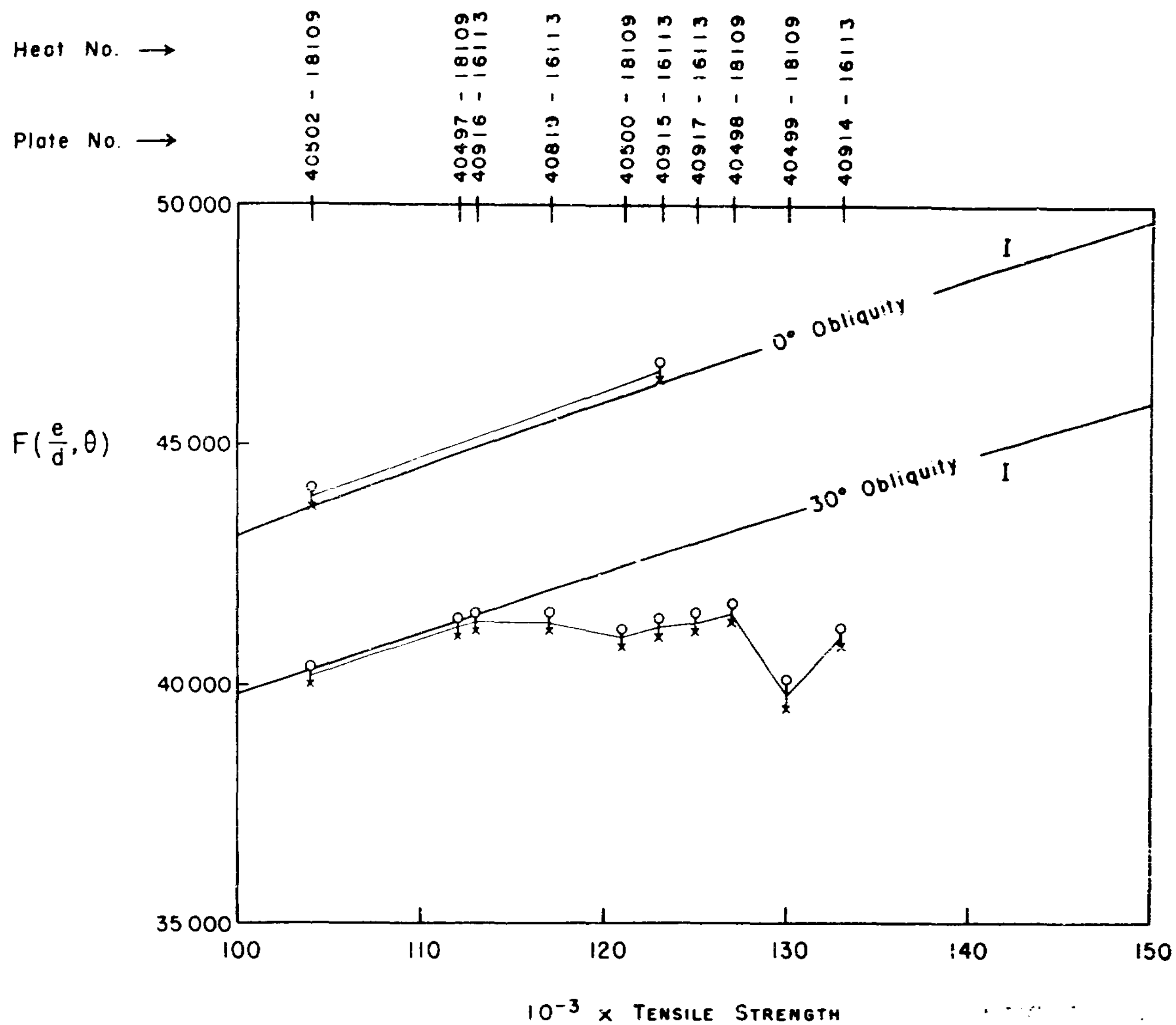

Complete Penetration, estimated minimum value

Incomplete Penetration, estimated maximum value

e/d = 5

UNCLASSIFIED

PG PHOTO NO 2990 (APL) [redacted] FIGURE (20)

PLATE PENETRATION COEFFICIENTS

3" AP M79 Projectile vs CI Plates No. 40502 and 40915

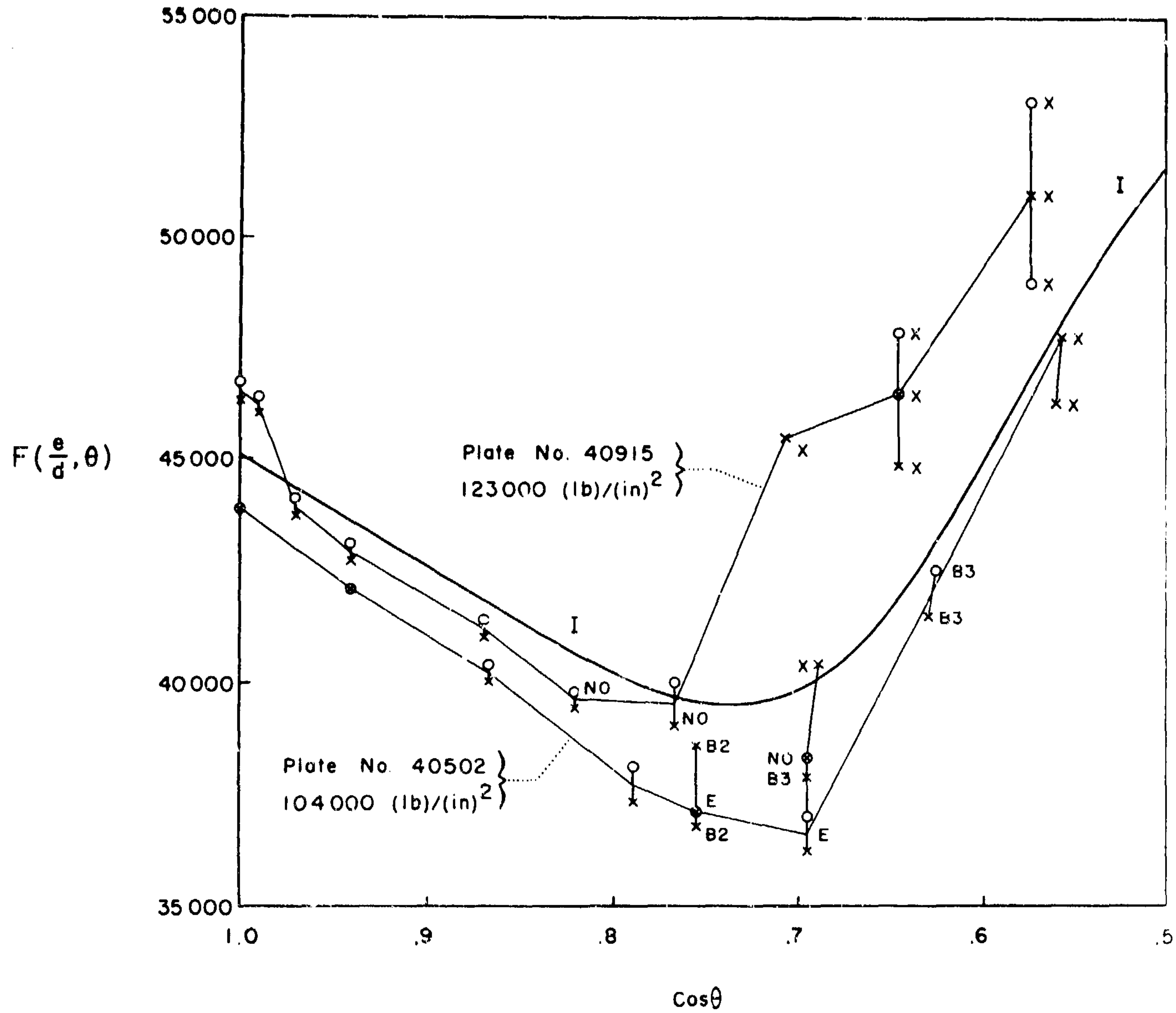

e/d = .5

PROJECTILE CONDITION

E = Undeformed

NO = Nose Offset

B2 = Broken in Two

X = Shattered

Complete Penetration, estimated minimum value

Incomplete Penetration, estimated maximum value

UNCLASSIFIED

[redacted]

NPG PHOTO NO 2991 (APL)

FIGURE (21)

PLATE PENETRATION COEFFICIENTS

3" AP M79 Projectile vs CI Plates No. 59533 and 87207

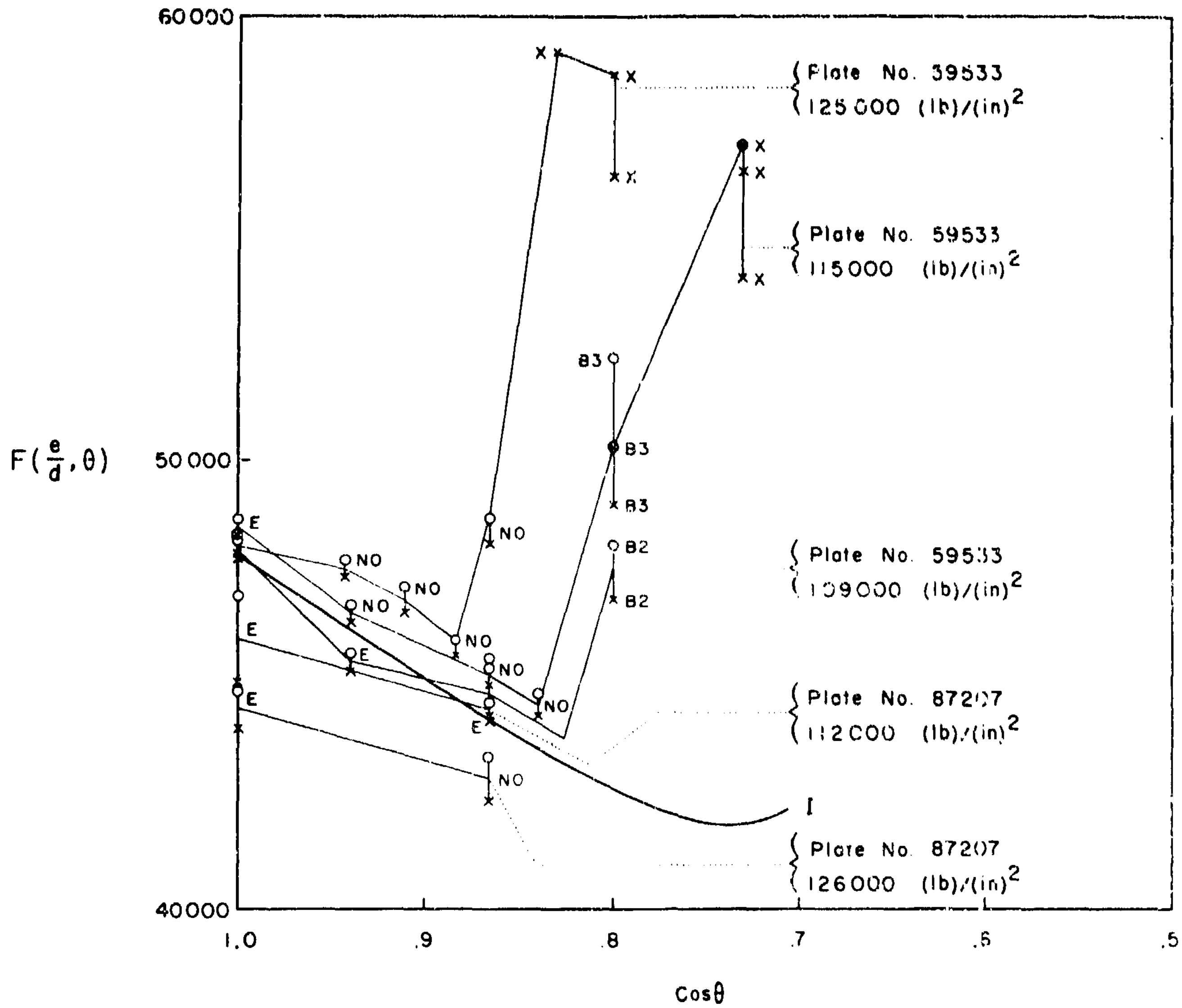

PROJECTILE CONDITION

E = Undeformed

NO = Nose Offset

B2 = Broken in Two

X = Shattered

$e/d = .32$

Complete Penetration, estimated minimum value

Incomplete Penetration, estimated maximum value

UNCLASSIFIED

NPG PHOTO NO 2992 (APL) [redacted] FIGURE (22)

PLATE PENETRATION COEFFICIENTS

Uncapped 3" Projectiles vs CI Plate No. 55909 of 119000 (lb)/(in)^2 Tensile Strength

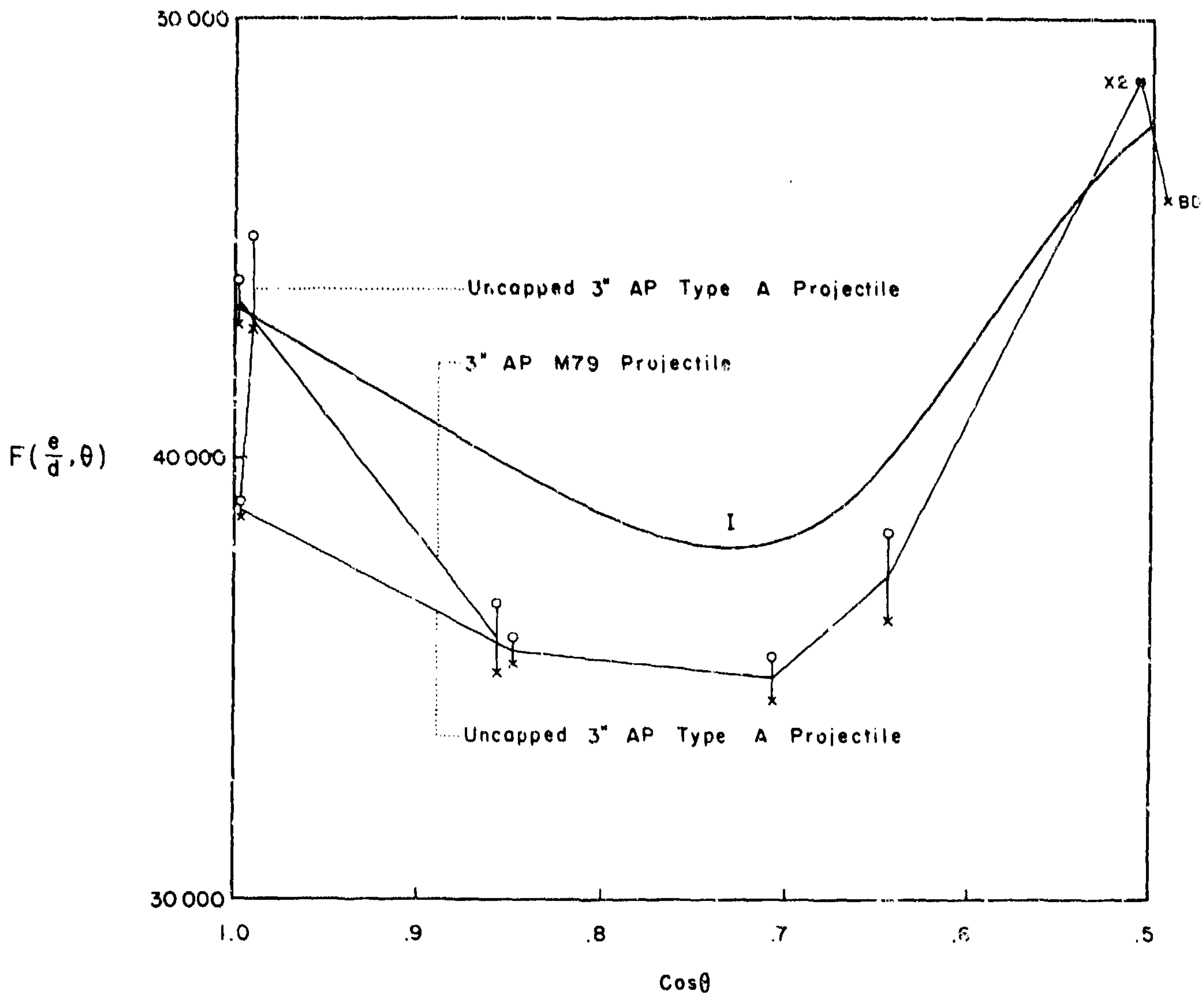

PROJECTILE CONDITION

BD = Base Dented

X2 = Split in Two

e/d = .41

Complete Penetration, estimated minimum value

Incomplete Penetration, estimated maximum value

UNCLASSIFIED

NPG PHOTO NO. 2993 (APL) [redacted] FIGURE (23)

THE DYNAMIC TENSILE STRENGTHS OF SEVERAL STEELS

Strain Rate = 200 (sec)$^{-1}$

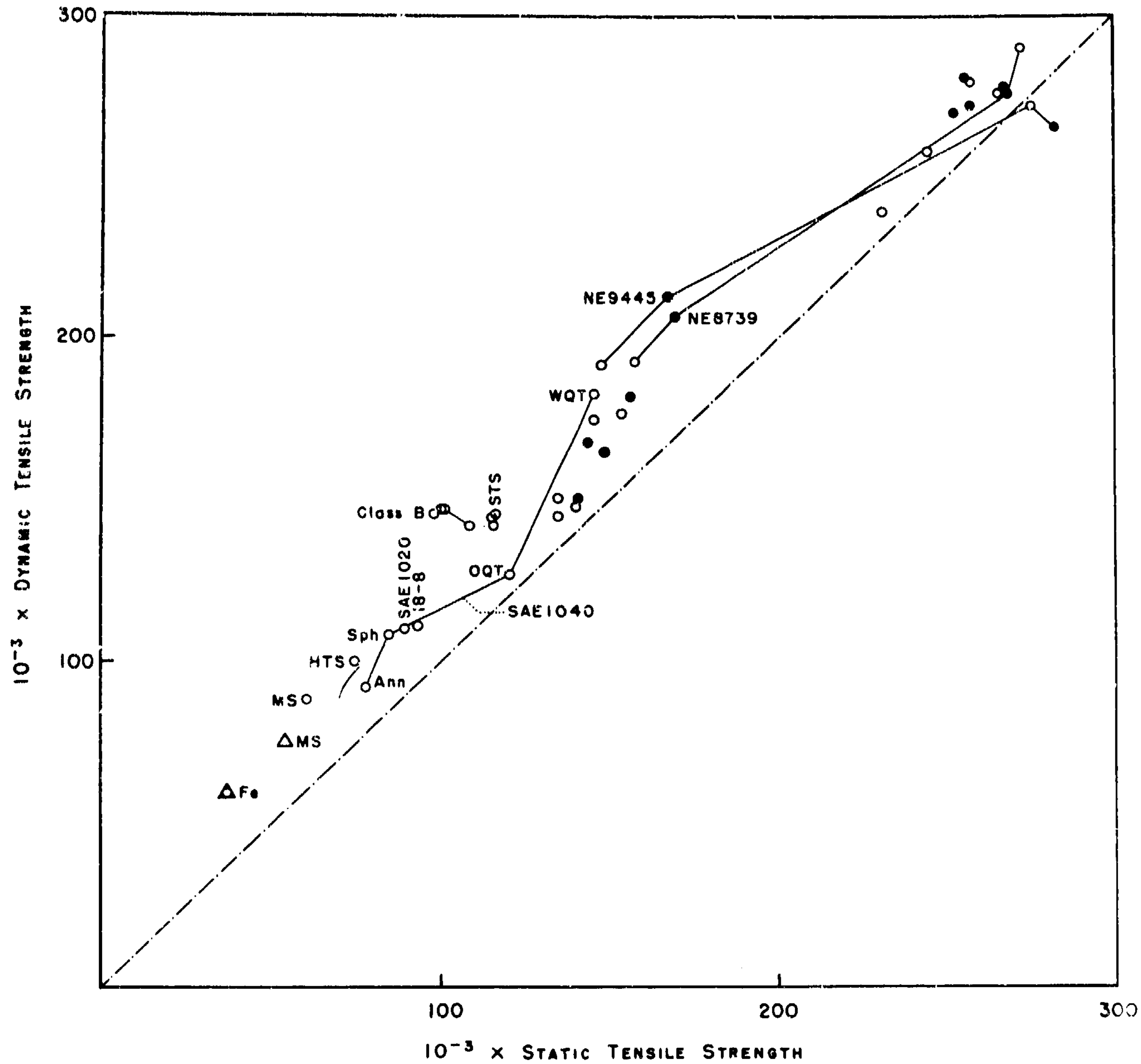

Fe = Pure Iron
MS = Mild Steel
HTS = High Tensile Steel
STS = Special Treatment Steel
Ann = Annealed
Sph = Spheroidized
OQT = Oil Quenched and Tempered
WQT = Water Quenched and Tempered

△ Westinghouse Research Laboratory Data

○ California Institute of Technology Data Quenched and Tempered Steel

● California Institute of Technology Data Austempered Steel